TRANSLATION SURFACES: SADDLE CONNECTIONS, TRIANGLES AND COVERING CONSTRUCTIONS

A Dissertation

Presented to the Faculty of the Graduate School

of Cornell University

in Partial Fulfillment of the Requirements for the Degree of

Doctor of Philosophy

by

Chenxi Wu

August 2016

TRANSLATION SURFACES: SADDLE CONNECTIONS, TRIANGLES AND COVERING CONSTRUCTIONS

Chenxi Wu, Ph.D.

Cornell University 2016

In these thesis we prove 3 results on the dynamics of translation surfaces. Firstly, we show that the set of the holonomy vectors of saddle connections on a lattice surface can not satisfy the Deloné property. Smillie and Weiss showed that every lattice surface has a triangle and a virtual triangle of the minimal area. We calculate the area of the smallest triangle and virtual triangle for many classes of lattice surfaces, and describe all lattice surfaces for which the area of virtual triangle is greater than an explicit constant. Many interesting examples of translation surface can be obtained through deforming abelian covers of the pillowcase. We calculate the action of affine diffeomorphism group on the relative cohomology of an abelian cover of the pillowcase, extending the previous calculation. Lastly, we use this calculation to give a characterization of the Bouw-Möller surfaces.

BIOGRAPHICAL SKETCH

Chenxi Wu was born and raised in Guangzhou, China.,He did undergraduate studies in Mathematics at Peking university from 2006-2010, and began graduate studies in Mathematics at Cornell University in August 2010.

This thesis is dedicated to my teachers, classmates, and friends.

ACKNOWLEDGEMENTS

I warmly thank his thesis advisor John Smillie for his great contribution of knowledge, ideas, funding and time. I also greatly thank Alex Wright, Barak Weiss, Gabriela Schmithüsen and Anja Randecker for many interesting conversations and lots of help.

TABLE OF CONTENTS

LIST OF TABLES

LIST OF FIGURES

CHAPTER 1

INTRODUCTION

The study of the flat torus is a classical subject, going back to at least the 1880s; however, the extensive study of the geometry and dynamics on general translation surfaces and their strata is more recent. An early work in this field is the paper of Fox and Kershner [23]. Since the 80's, the dynamics of translation surfaces has been studied by Earle, Gardiner, Kerckhoff, Masur, Smillie, Veech, Thurston, Vorobets, Eskin, Mirzahani, Wright, and many more. Some expository papers on this subject are [59] by Zorich and [57] by Wright.

The dynamics of geodesics on translation surfaces is related to interval exchange transformation (IET) [33] as well as the dynamics of rational billiards [52]. It also has interesting connections with algebraic geometry and number theory. To study geodesics on a translation surface, it is often useful to consider the affine, $GL(2,\mathbb{R})$-action on the moduli spaces of translation surfaces. The stratum consisting of translation surfaces of a given combinatorial type has the structure of an affine manifold with respect to charts given by the period coordinates. This affine structure is compatible with a natural measure invariant under the $SL(2,\mathbb{R})$-action. Furthermore, the $SL(2,\mathbb{R})$-action is ergodic under this invariant measure when restricting to the part of unit area [33], which has a variety of applications. For example, this ergodicity provides a way of estimating the growth rate of the finite geodesics (saddle connections) on a generic translation surface, through the

volume of this invariant measure on strata restricting to the hypersurface of translation surfaces of unit area [16, 18]. This $SL(2,\mathbb{R})$-action also has other invariant ergodic measures supported on certain proper affine submanifolds of the strata [19]. For example, there are those supported on a single closed orbits, whose elements are called lattice surfaces. Below is a more detailed overview of a few topics in the dynamics of translation surfaces.

- **Lattice Surfaces:** Lattice surfaces are translation surfaces whose affine diffeomorphisms have derivatives that generate a lattice in $SL(2,\mathbb{R})$.

  The flat torus is an example of a lattice surface. One technique of constructing lattice surfaces is through a finite cover or branched cover of another lattice surface. Lattice surfaces arising out of a covering construction on the flat torus are called square-tiled, or arithmetic, lattice surfaces. These surfaces have been studied by Schmithüsen, Hubert, Forni, Matheus, Yoccoz, Zorich, Wright and many others, and are useful for the calculation of the volume and Siegel-Veech constants of the strata.

  The first class of non-squared tiled lattice surfaces was discovered by Veech [52]. Other interesting families of non-square-tiled lattice surfaces that have been discovered since then include: eigenforms in $\mathcal{H}(2)$, found by McMullen [39] and Calta [8] (); lattice surfaces in the Prym eigenform loci of genus 3

and 4 found by McMullen [40]; the family found by Ward [54], and more generally, the Bouw-Möller family [6]; isolated examples found by Vorobets [53], Kenyon-Smillie [29]. Furthermore, there are two new infinite families of lattice surfaces in the forthcoming works of McMullen-Mukamel-Wright and Eskin-McMullen-Mukamel-Wright. Not many classification results on lattice surfaces is fully known. McMullen [39] also classified all the genus 2 lattice surfaces.

Smillie showed that lattice surfaces are the translation surfaces whose $GL(2,\mathbb{R})$ orbits in their strata are closed, cf. [48]. These closed $GL(2,\mathbb{R})$-orbits are called Teichmüller curves. According to [19], all $GL(2,\mathbb{R})$-orbit closures in the strata are affine submanifolds, hence Teichmüller curves are the orbit closures of the lowest possible dimension. Kenyon-Smillie [29], Bainbridge-Möller [4], Bainbridge-Habegger-Möller [3], Matheus-Wright [36], Lanneau-Nguyen-Wright [31] and others established finiteness results of Teichmüller curves in many different settings. The forthcoming work of Eskin-Filip-Wright establishes finiteness result that is very powerful.

- **Higher-dimensional Orbit Closures:** It is interesting for many reasons to understand higher dimensional orbit closures and invariant measures of the $SL(2, athbbR)$-action. The connected components of the strata are orbit closures, and higher-dimensional orbit closures can also be obtained from a covering construction, which has been studies in e.g. [17, 15]. The seminal

work of Eskin-Mirzahani-Mohammadi [19] showed that all orbit closures of the $GL(2,\mathbb{R})$-action are affine submanifolds.

Some of the first higher-dimensional orbit closures that are neither connected components of the strata, nor arise from a covering construction, were found by McMullen [41, 40] and Calta [8]. More have been found by Eskin, McMullen, Mukamel and Wright.

- **Horocycle Orbit Closures and Ergodic invariant measures:** The study of ergodic invariant measures of the horocycle flow is related to the question of the growth rate of saddle connections on an arbitrary translation surface. Smillie-Weiss [48] characterized all minimal sets of this flow, and more complicated orbit closures and invariant measures of this flow have been found and studied by Bainbridge, Smillie, Weiss, Clavier etc. In particular, Bainbridge-Smillie-Weiss [5] classified all horocycle orbit closures and ergodic invariant measures in the eigenform loci in $\mathcal{H}(1,1)$. This is closely related to the study of the real *rel* foliation, which has been studied by Minsky-Weiss[43], McMullen [42] and others.

- **Saddle Connections:** Another topic that has been extensively studied is the holonomies of the saddle connections on a translation surface. It is known that the growth rate of this set does satisfy such upper and lower bounds by [34] and [35]. For some translation surfaces the asymptotic upper and

lower bounds agree. Veech [52], Eskin and Masur [16] showed that this is the case for Veech surfaces and generic translation surfaces respectively. Also, whether or not the translation surface is a lattice surface is determined by properties of the growth rate of the holonomies of the saddle connections as shown in Smillie and Weiss [49]. Furthermore, additional properties that the set of holonomies of the saddle connections has to satisfy are contained in the works of Athreya and Chaika [1, 2] on the distribution of angles between successive saddle connections of bounded length.

Figure 1.1 is a plot of the set of holonomy vectors of saddle connections on a lattice surface in $\mathcal{H}(2)$ corresponding to the quadratic order of discriminant 13, as defined in [41].

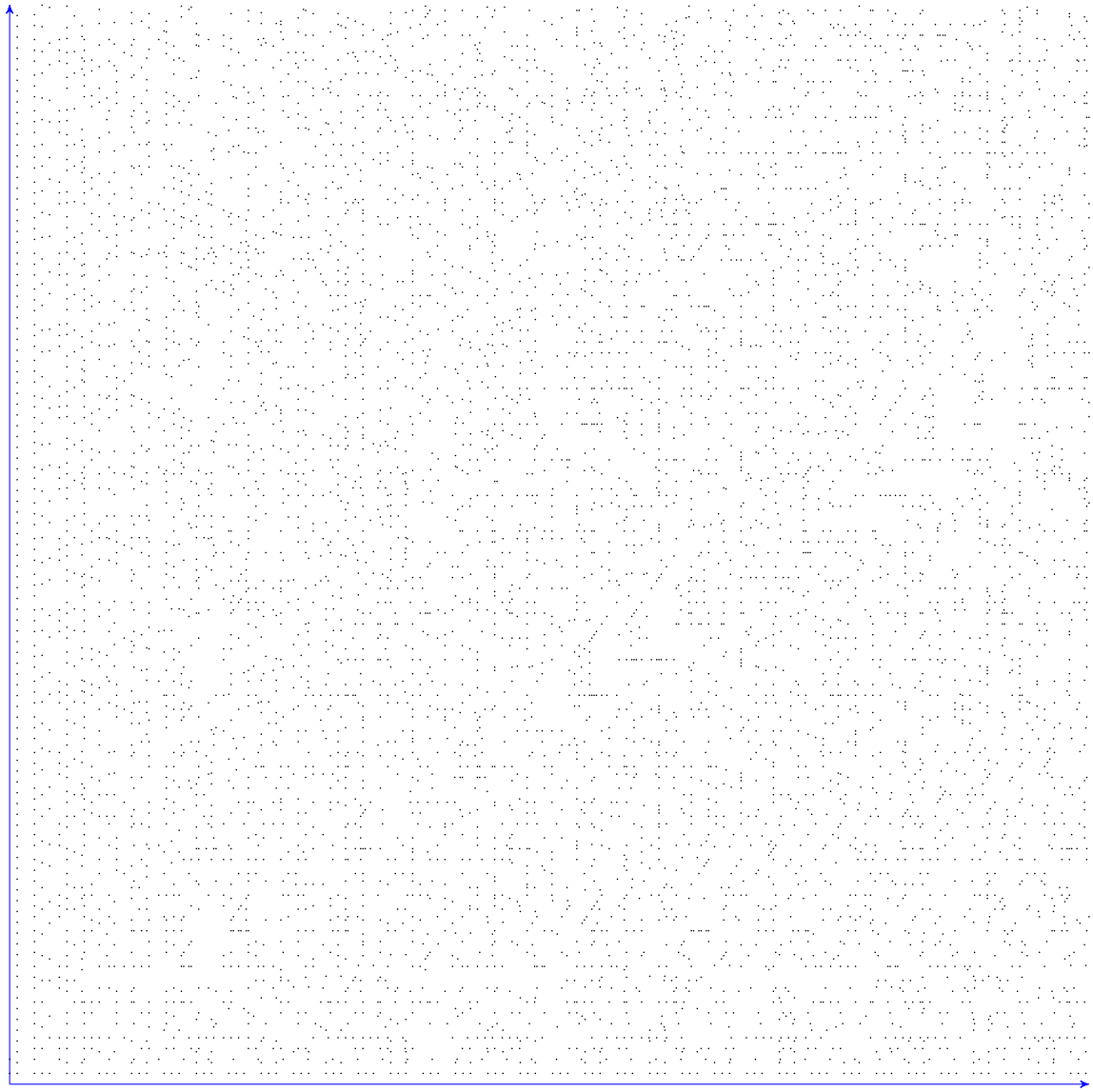

Figure 1.1: holonomy vectors of saddle connections on a lattice surface in $\mathcal{H}(2)$ corresponding to the quadratic order of discriminant 13

In this thesis, we will answer a few specific questions on the dynamics of flat surfaces.

- In Chapter 2, we will review some concepts and properties about translation surfaces.
- In Chapter 3, we answer a question by Barak Weiss on the uniform discreteness of the holonomies of saddle connections by constructing translation surfaces where the set of holonomies of the saddle connections is not uniformly discrete. See Theorem 3.0.2.
- In Chapter 4, we use the area of smallest triangle and virtual triangle, defined by Smillie-Weiss [49], to study lattice surfaces. We calculate these areas for some classes of known lattice surface (Theorem 4.1.2-4.1.5), and carry out the algorithm that enumerate lattice surfaces described in [49] in the case where the area of smallest virtual triangle is larger than .05 (Theorem 4.1.1).
- In Chapter 5, we calculate the action of the affine diffeomorphism groups on a class of square-tiled lattice surfaces (Theorem 5.1.1, 5.1.3), which has an application in the construction of horocycle orbit closures.
- In Chapter 6, we use the idea from Chapter 5 to give a more geometric description of the Bouw-Möller surfaces (Theorem 6.1.1), following the works of Bouw-Möller [6], Hooper [27] and Wright [56].

CHAPTER 2

BACKGROUND

A *translation surface (of finite area and genus) M* is a compact connected surface with a *translation structure*, i.e. an atlas that covers M except for finitely many points for which the transition functions are translations. In other words, it is a compact Riemann surface with a holomorphic differential. The zeros of this holomorphic differential are called *cone points*, and the degree of a zero is called its degree. A line segment that ends in cone point(s) is called a *saddle connection*. Sometimes we will also consider translation surfaces with finitely many marked points, which can be seen as a cone point of order 0. All translation surfaces we deal with in this thesis are assumed to be of finite genus and area.

Given a n-tuple of non-negative integers $k = (k_1, \dots k_n)$, $\mathcal{H}(k)$ is the set of all translation surfaces with n cone points or marked points, with orders $k_1, \dots k_n$. We denote by Σ the set consisting of these points. $\mathcal{H}(k)$ has a topology induced by being a subspace of the cotangent bundle of the moduli space $\mathcal{M}_{\frac{1}{2}\sum_i k_i+1}$. It has an atlas called the *period coordinate*, which consists of coordinate charts that send a translation surface M to an element in $H^1(M, \Sigma; \mathbb{C}) = Hom(H_1(M, \Sigma; \mathbb{Z}), \mathbb{C})$, which sends each element in $H_1(M, \Sigma; \mathbb{Z})$, represented by a path γ, to its holonomy under the translation structure. This atlas gives $\mathcal{H}(k)$ the structure of an affine manifold.

The group $GL(2,\mathbb{R})$ acts on $\mathcal{H}(k)$ by post-composing with the charts that define the translation structure. The orbit closures of this action is an affine submanifold, which is proved in [19]. When the closure consists of a single orbit, it is called a *Teichmüller curve*, and its elements are *Lattice surfaces* because their Veech groups are lattices. Here the Veech group of a translation surface is the discrete subgroup of $SL(2,\mathbb{R})$ consisting of the derivatives of its affine automorphisms. These surfaces can be seen as the generalization of the flat torus, and their geometric and dynamical properties have been extensively studied. For example, Veech [52] showed that the growth rate of the holonomies of saddle connections in any Veech surface must be asymptotically quadratic. He also proved the Veech dichotomy, which says that the translation flow in any given Veech surface must be either uniquely ergodic or completely periodic.

CHAPTER 3

THE DELONÉ PROPERTY OF HOLONOMIES OF SADDLE CONNECTIONS

For a translation surface M, let $S_M \subset \mathbb{R}^2$ be the set of holonomy vectors of all saddle connections of M. The set S_M is discrete, the directions of vectors in S_M are dense, and the growth rate of S_M (the number of points within radius R of the origin) admits quadratic upper and lower bounds [34, 35].

Another way of capturing the concept of uniformity of a subset of a metric space is the concept of a Deloné set.

Definition 3.0.1. [45] A subset A of a metric space X is a Deloné set if:

1. A is relatively dense, i.e. there is $R > 0$ such that any ball of radius R in X contains at least one point in A.
2. A is uniformly discrete, i.e. there is $r > 0$ such that for any two distinct points $x, y \in A$, $d(x, y) > r$.

The Deloné property is stronger than the existence of a quadratic upper and lower bound on the growth rate. For example, in the case of the flat torus, it is a classical result that S_M is not relatively dense, hence not Deloné, due to the Chinese remainder theorem, c.f. [26] or Theorem 3.0.5 below.

Barak Weiss asked for which translation surfaces M, is S_M a Deloné set. Here, we will show that:

Theorem 3.0.1. *If M is a lattice surface then S_M is never a Deloné set. On the other hand, there exists a non-lattice translation surface M for which S_M is a Deloné set.*

A square-tiled surface is a lattice surface because it is a finite branched cover of the flat torus branched at one point. We will show that if lattice surface M is a not square-tiled, i.e. non-arithmetic, then S_M cannot be uniformly discrete. We will also show that if M is square-tiled then S_M cannot be relatively dense. Combining these two results, we can conclude that when M is a lattice surface, S_M cannot be a Deloné set.

Theorem 3.0.2. *If M is a non-arithmetic lattice surface, then S_M is not uniformly discrete.*

Proof. Let M is a non-arithmetic lattice surface and let $r > 0$ be given. By [52] we can choose a periodic direction γ of M such that in this direction M is decomposed into cylinders $C_1, \ldots, C_n$ in the direction of γ, and the width of all these cylinders are no larger than $r/4$. Because M is a lattice surface, the holonomy field [29] is generated by the ratios of the circumferences. Because M is not square-tiled, the holonomy field can not be $\mathbb{Q}$. Hence, there exist two numbers i and j such that the quotient of the circumferences of C_i and C_j is not in $\mathbb{Q}$. Denote the holonomy vectors of periodic geodesics corresponding to C_i and C_j by l and l'. Let h and h'

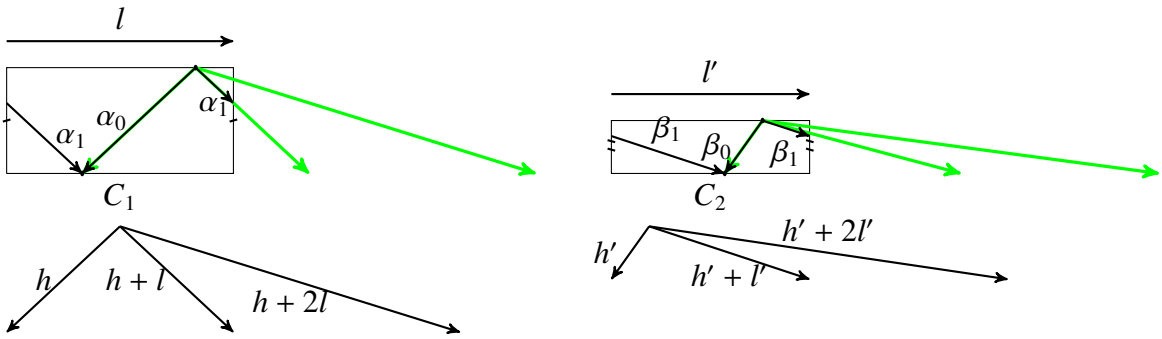

Figure 3.1: The figure on the left shows C_1, a saddle connection α_0 that crosses C_1, and its image α_1 under a Dehn twist. Let h be the holonomy of α_0, and let l be the circumference of C_1, then the holonomy of α_1 is $h + l$. Similarly, the image of α_0 under the k-th power of the Dehn twist, which is denoted by α_k, has holonomy $h+kl$. These holonomy vectors are shown below the corresponding cylinders. The figure on the right shows the the same for C_2, whose circumference l' is irrationally related to l.

be the holonomy vectors of two saddle connections α_0 and β_0 crossing C_i and C_j respectively. Let α_n be the images of α_0 under n-Dehn twists in cylinders C_i, β_n be the image of β_0 under n-Dehn twists in cylinder C_j. Given $n \in \mathbb{Z}$, both α_n and β_n are still saddle connections of M. Thus, for any integer n, the vectors $h + nl$ and $h' + nl'$ are in S_M, as in Figure 3.1.

Let us write h as $h = h_1 + h_2$ and h' as $h' = h'_1 + h'_2$, where h_1 and h'_1 are vectors in direction γ, and h_2 and h'_2 are vectors in direction $\gamma^\perp$. Because the widths of C_i and C_j are no larger than $r/4$ by assumption, $\|h_2 - h'_2\| < r/2$. Because h_1, h'_1, l and l' are vectors pointing in the same direction, we can write $h_1 = al$, $h'_1 = bl$, $l' = \lambda l$. Let $l' = \lambda l$. Because λ is irrational, the set $\{m + m'\lambda : m, m' \in \mathbb{Z}\}$ is dense in $\mathbb{R}$, so there exists a pair of integers n_0 and n'_0 such that $|a - b + n_0 - n'_0\lambda| < \frac{r}{2\|l\|}$. Thus

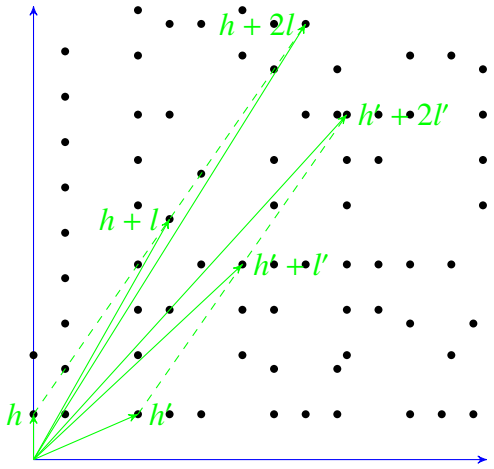

Figure 3.2: Some $h + kl$ and $h' + kl'$ in Figure 1.1.

$\|(h_1 + n_0 l) - (h'_1 + n'_0 l')\| < r/2$, and $\|(h + n_0 l) - (h' + n'_0 l')\| < r/2 + r/2 = r$. We conclude that S_M contains two points for which the distance between them is less than any $r > 0$, thus S_M is not uniformly discrete. □

The above argument also works on those completely periodic surfaces such that in any given periodic direction, there are at least two closed geodesics whose length are not related by a rational multiple. Furthermore, Barak Weiss pointed out that the proof above can be generalized into the following:

Theorem 3.0.3. *(Weiss) The orbit of any point* $p \in \mathbb{R}^2 - (0,0)$ *under a non-arithmetic lattice* Γ *in* $SL(2,\mathbb{R})$ *is not uniformly discrete.*

Proof. If Γ is cocompact then the Γ orbit is dense. This result is standard, see e.g. [10]. If Γ is non-uniform then Γ must contain two non-commuting parabolic elements. By conjugating Γ, we can assume that these elements are $\gamma_1 : (x, y) \mapsto$

$(x, y + x)$ and $\gamma_2 : (x, y) \mapsto (x + y, y)$. Because Γ is not arithmetic, Γp is not contained in a lattice in $\mathbb{R}^2$, hence its projection on to the x or y axis is not in $\mathbb{Z}\epsilon$ for any ϵ. It follows that there are points $(x_1, y_1), (x_2, y_2) \in \Gamma p$ such that $x_1/x_2 \notin \mathbb{Q}$ or $y_1/y_2 \notin \mathbb{Q}$. Suppose $x_1/x_2 \notin \mathbb{Q}$, then given any $r > 0$, there is a pair of integers $m, n \in \mathbb{Z}$ such that $0 < |(y_1 + mx_1) - (y_2 + nx_2)| < r/2$. Let M be an integer such that $0 < |x_2 - x_1 - M((y_1 + mx_1) - (y_2 + nx_2))| \leq r/2$, then the distance between distinct points $\gamma_2^M \gamma_1^m (x_1, y_1)$ and $\gamma_2^M \gamma_1^n (x_2, y_2)$ in Γp is smaller than r. The same argument works for the case when $y_1/y_2 \notin \mathbb{Q}$. □

Remark 3.0.1. The proof above shows that as long as Γ contain two non-commuting unipotent elements, any Γ-orbit is either contained in a lattice or not uniformly discrete. Theorem 3.0.3 implies Theorem 3.0.2 if we choose p to be the holonomy of a saddle connection and Γ as the Veech group.

Now we deal with the square-tiled case. This case is closely related to the classical case of the torus discussed in [26]. In this case, $S_M = \{(p, q) : \gcd(p, q) = 1\}$

Lemma 3.0.4. *For any positive integer N, the set $\{(p, q) \in \mathbb{Z}^2 : \gcd(p, q) \leq N\}$ is not relatively dense in $\mathbb{R}^2$.*

Proof. ([26]) Given $R > 0$, choose an integer $n > 2R$, and n^2 distinct prime numbers $p_{i,j}$, $1 < i, j < n$ larger than N. Let $q_i = \prod_j p_{i,j}$ and $q'_j = \prod_i p_{i,j}$. By the Chinese remainder theorem there is an integer x such that for all i, $x \equiv -i \mod q_i$, and an integer y such that for all j, $y \equiv -j \mod q'_j$. Hence for any two positive integers

$i, j \leq n$, $(x+i, y+j) \in \{(p,q) \in \mathbb{Z}^2 : \gcd(p,q) > N\}$. In particular, there is a ball in $\mathbb{R}^2$ of radius R that does not contain points in the set $\{(p,q) \in \mathbb{Z}^2 : \gcd(p,q) \leq N\}$. □

Now we use the above lemma to show that if the surface M is square-tiled, S_M cannot be relatively dense.

Theorem 3.0.5. *If M is a square-tiled lattice surface then S_M is not relatively dense in $\mathbb{R}^2$.*

Proof. If M is square-tiled, we can assume that M is tiled be 1×1 squares. Let N be the number of squares that tiled M, then M is an n-fold branched cover of $T = \mathbb{R}^2/\mathbb{Z}^2$ branched at $(0,0)$. Therefore, the holonomy of any saddle connection is in $\mathbb{Z} \times \mathbb{Z}$. For any pair of coprime integers (p,q), let γ be the closed geodesic in T starting at $(0,0)$ whose holonomy is (p,q). The length of γ is $\sqrt{p^2+q^2}$. The preimage of γ in M is a graph Γ. The vertices of Γ are the preimages of $(0,0)$, while edges are the preimages of γ. The sum of the lengths of the edges of Γ is $N\sqrt{p^2+q^2}$. Any saddle connection of M in (p,q)-direction is a path on Γ without self intersection, hence The length of such a saddle connection can not be greater than $N\sqrt{p^2+q^2}$. Hence, the holonomy of such a saddle connection is of the form (sp, sq), $s \in \mathbb{Z}$ with $|s| \leq N$. Thus, $S_M \subset \{(p,q) \in \mathbb{Z}^2 : \gcd(p,q) \leq N\}$, so by Lemma 3.0.4 S_M is not relatively dense in $\mathbb{R}^2$. □

Remark 3.0.2. It has been pointed out to the author that Lemma 3.0.4 implies that the $SL(2,\mathbb{Z})$ orbit of a finite set of points $X \subset \mathbb{Z}^2$ is not uniformly dense.

Finally, when M is not a lattice surface, S_M *can* be a Deloné set, which we will show in Example below. This construction finishes the proof of Theorem 3.0.1.

Example. Let M_1 be the branched double cover of $\mathbb{R}^2/\mathbb{Z}^2$ branched at points $(0,0)$ and $(\sqrt{2}-1, \sqrt{3}-1)$. Let $\tilde{M}$ be a $\mathbb{Z}^2$-cover which is a branched double cover of $\mathbb{R}^2$ branched at $U = \mathbb{Z}^2$ and at $V = \mathbb{Z}^2 + (\sqrt{2}-1, \sqrt{3}-1)$, where the deck group action is by translation. Then saddle connections on M_1 lift to saddle connections on $\tilde{M}$, and any two lifts have the same holonomy, hence S_{M_1} is the same as $S_{\tilde{M}}$, which is the set of holonomies of line segments linking two points in $W = U \cup V$ which do not pass through any other point in W. If a line segment links two points in U, its slope must be rational or ∞, hence it would not pass through any point in V. Furthermore, it does not pass through any other point in U if and only if its holonomy is a pair of coprime integers. The same is true for line segments linking two points in V. On the other hand, given any point $p \in U$ and any point $q \in V$, a line segment from p to q has irrational slope hence cannot pass through any other point in U or V, therefore the holonomy of such line segment can be any vector in $\mathbb{Z}^2 + (\sqrt{2}-1, \sqrt{3}-1)$. Similarly the holonomies of saddle connections from V to U are $\mathbb{Z}^2 - (\sqrt{2}-1, \sqrt{3}-1)$. Hence $S_{M_1} = \{(a,b) \in \mathbb{Z}^2 : \gcd(a,b) = 1\} \cup (\mathbb{Z}^2 + (\sqrt{2}-1, \sqrt{3}-1)) \cup (\mathbb{Z}^2 - (\sqrt{2}-1, \sqrt{3}-1))$, this set is uniformly discrete, and the last two pieces are uniformly dense.

□

The set S_M is still far from being fully understood. For example, it would be

interesting to know the answer to these questions:

1. Can the set of holonomy vectors of all saddle connections of a non-arithmetic lattice surface be relatively dense?
2. Is there any characterization of the set of flat surfaces M such that S_M are Deloné, relatively dense or uniformly discrete?
3. Is there a surface M which is not a branched cover of the torus for which S_M is Deloné?

CHAPTER 4

MINIMAL AREA OF TRIANGLES AND VIRTUAL TRIANGLES

4.1 Introduction

A natural way to characterize the complexity of a square-tiled surface is by considering the minimal number of squares needed to construct this surface. Analogously, for more general lattice surfaces, Vorobets [53], Smillie and Weiss [49] established the existence of a lower bound of the area of an embedded triangle formed by saddle connections. This minimal area also characterizes the complexity of the surface in an analogous sense. In particular, if a surface M is tiled by N squares, the minimal area of an embedded triangle formed by saddle connections must be at least $\frac{1}{2N}$ of the total area. Hence, for a lattice surface M, we define the minimal area of triangle $Area_T(M) = \inf\{Area_\Delta\}/Area(M)$, where $\inf\{Area_\Delta\}$ is the minimal area of embedded triangles formed by saddle connections, and $Area(M)$ is the total area of the surface.

Furthermore, Smillie and Weiss [49] showed that given $\epsilon > 0$, any flat surface with $Area_T > \epsilon$ lies on one of finitely many Teichmüller curves. From this, they developed an algorithm to find all lattice surfaces and list them in order of complexity.

A related notion introduced in [49] is the minimal area of a virtual triangle, defined as $Area_{VT}(M) = \frac{1}{2}\inf_{l,l'} ||l \times l'||/Area(M)$, where l and l' are holonomies of non-parallel saddle connections, and $Area(M)$ is the total area of the surface. Smillie and Weiss [49] gave the first six lattice surfaces obtained by their algorithm. Samuel Leliévre found further examples and showed that it is interesting to plot $Area_T$ against $Area_{VT}$. Yumin Zhong [58] showed that the double regular pentagon has the smallest $Area_T$ among non-arithmetic lattice surfaces.

In this chapter, we calculate the quantities $Area_T$ and $Area_{VT}$ of all published primitive lattice surfaces except those in the Prym eigenform loci of $\mathcal{H}(6)$. We also provide a list of the Veech surfaces with $Area_{VT} > 0.05$.

In section 4.3, we calculate all the lattice surfaces with $Area_{VT} > 0.05$ using the method outlined in [49] with some improvements which we describe there. This method will eventually produce all lattice surfaces in theory, but the amount of computation may grow very fast as the bound on $Area_{VT}$ decreases. We show that the published list of lattice surfaces is complete up to $Area_{VT} > 0.05$. More specifically, we show the following:

Theorem 4.1.1. *The following is a complete list of lattice surfaces for which* $Area_{VT}(M) > 0.05$*:*

(1) Square-tiled surfaces having less than 10 *squares. These are included in the "origami*

database" in [11] by Delecroix, there are of 315 of them up to affine transformation.

(2) *Lattice surfaces in* $\mathcal{H}(2)$ *with discriminant* 5, 8 *or* 17. *There are 4 of them up to affine transformation.*

(3) *Lattice surfaces in the Prym eigenform loci in* $\mathcal{H}(4)$ *with discriminant* 8. *There is only 1 lattice surface of this type up to affine transformation.*

There are two Teichmüller curves in $\mathcal{H}(2)$ that have discriminant 17, so there are five different non-arithmetic lattice surfaces up to affine action that have $Area_{VT} > 0.05$.

Together with the calculation on square-tiled surfaces done by Delecroix [11], the numbers of surfaces for each given $Area_{VT} > 0.05$, up to affine transformation, are calculated and summarized in Table 4.1.

Table 4.1: Lattice surfaces with $Area_{VT} > 0.5$

$Area_{VT}$	num. of surfaces	
1/2	1	flat torus
1/6	1	square tiled
1/8	3	square tiled
1/10	7	square tiled
0.0854102	1	double regular pentagon
1/12	25	square tiled
0.0732233	1	regular octagon
1/14	40	square tiled
1/16	113	square tiled
1/18	125	square tiled
0.0531695	2	genus 2 lattice surface with discriminant 17
0.0517767	1	Prym surface in genus 3 with discriminant 8, which is also the Bouw-Möller surface $BM(3,4)$

In Section 4.2, we calculate the $Area_T$ and $Area_{VT}$ of lattice surfaces in $\mathcal{H}(2)$, in the Prym loci of $\mathcal{H}(4)$, in the Bouw-Möller family, as well as in the isolated Teichmüller curves discovered by Vorobets [53] and Kenyon-Smillie [29]. Figures 4.1-4.2 show the $Area_T$ and $Area_{VT}$ of these lattice surfaces.

These results are summarized in the following theorems:

Theorem 4.1.2. *Let M be a lattice surface in $\mathcal{H}(2)$ with discriminant D. Then it holds:*

- *If D is a square,*

$$Area_T(M) = Area_{VT}(M) = \frac{1}{2\sqrt{D}}.$$

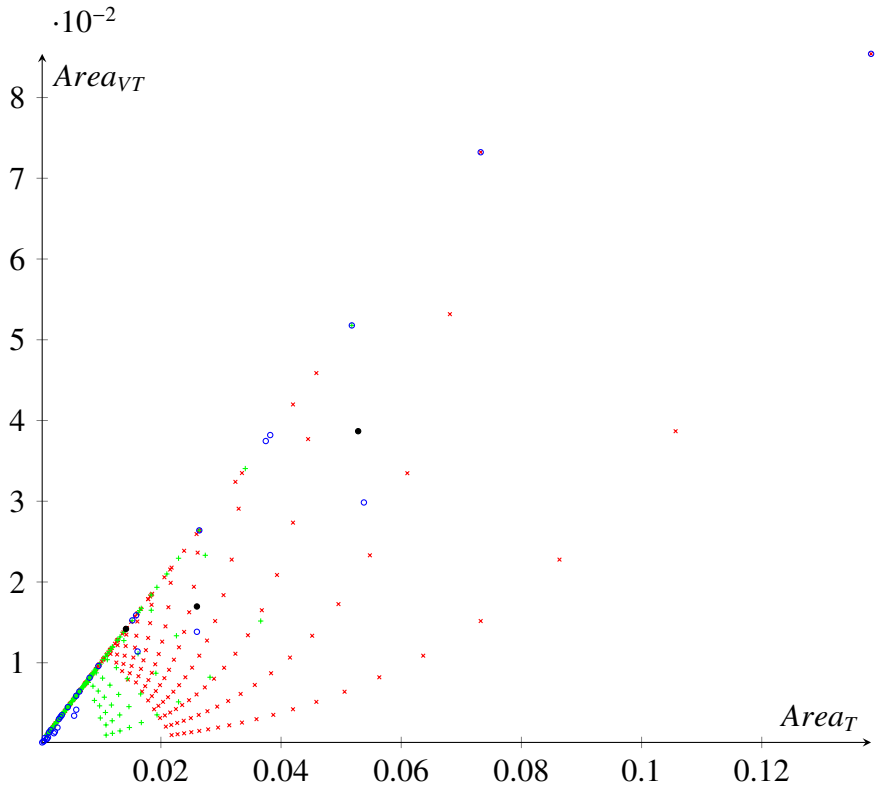

Figure 4.1: Red, green, blue and black points correspond to non-square-tiled lattice surfaces described in Theorem 4.1.2, 4.1.3, 4.1.4 and 4.1.5 respectively.

- *If D is not a square, let e_D be the largest integer satisfying $e_D \equiv D \mod 2$ and $e_D < \sqrt{D}$, then*

$$Area_T(M) = \frac{\sqrt{D} - e_D}{4\sqrt{D}}, \quad Area_{VT}(M) = \min\left(\frac{\sqrt{D} - e_D}{4\sqrt{D}}, \frac{2 + e_D - \sqrt{D}}{4\sqrt{D}}\right).$$

Theorem 4.1.3. *Let M be a lattice surface in the Prym locus in $\mathcal{H}(4)$ with discriminant D. Then:*

- *If D is a square,*

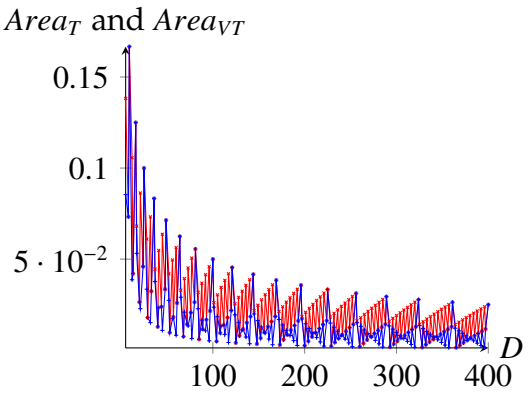

(a) Minimal area of triangle and virtual triangle of lattice surfaces in $\mathcal{H}(2)$ and their discriminant. Red is $Area_T$, blue is $Area_{VT}$.

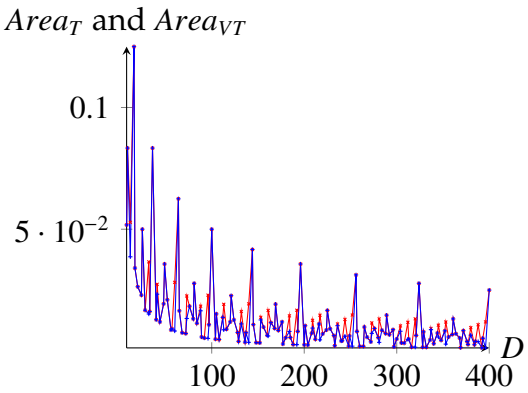

(b) Minimal area of triangle and virtual triangle of lattice surfaces in the Prym eigenform loci in $\mathcal{H}(4)$ and their discriminant. Red is $Area_T$, blue is $Area_{VT}$.

Figure 4.2: The pattern is related to the fractional part of the sequence $\sqrt{n}$.

- *If D is even,*

$$Area_T(M) = Area_{VT}(M) = \frac{1}{2\sqrt{D}}.$$

- *If D is odd,*

$$Area_T(M) = Area_{VT}(M) = \frac{1}{4\sqrt{D}}.$$

- *If D is not a square, denote by e'_D the largest integer satisfying ${e'_D}^2 \equiv D \mod 8$ and $e'_D < \sqrt{D}$, then:*

  - *If $\sqrt{D} - e'_D < 4/3$,*

$$Area_T(M) = Area_{VT}(M) = \frac{\sqrt{D} - e'_D}{8\sqrt{D}}.$$

  - *If $4/3 < \sqrt{D} - e'_D < 2$,*

$$Area_T(M) = \frac{\sqrt{D} - e'_D}{8\sqrt{D}}, Area_{VT}(M) = \frac{2 + e'_D - \sqrt{D}}{4\sqrt{D}}.$$

– *If* $2 < \sqrt{D} - e'_D < 8/3$,

$$Area_T(M) = Area_{VT}(M) = \frac{\sqrt{D} - e'_D - 2}{4\sqrt{D}}.$$

– *If* $\sqrt{D} - e'_D > 8/3$,

$$Area_T(M) = Area_{VT}(M) = \frac{4 - \sqrt{D} + e'_D}{8\sqrt{D}}.$$

Theorem 4.1.4. *The values* $Area_T$ *and* $Area_{VT}$ *of lattice surfaces in the Bouw-Möller family are as follows:*

- *If M is a regular n-gon where n is even,*

$$Area_T(M) = Area_{VT}(M) = \frac{4\sin\left(\frac{\pi}{n}\right)^2}{n}.$$

- *If M is a double n-gon where n is odd,*

$$Area_T(M) = \frac{2\sin\left(\frac{\pi}{n}\right)^2}{n}, \quad Area_{VT}(M) = \frac{\tan\left(\frac{\pi}{n}\right)\sin\left(\frac{\pi}{n}\right)}{n}.$$

- *If M is the Bouw-Möller surfaces* $S_{m,n}$, $\min(m,n) > 2$*:*

  Let

$$A = \sum_{k=1}^{n-1} \sin\left(\frac{k\pi}{n}\right)^2 \cdot \sum_{k=1}^{m-2} \sin\left(\frac{k\pi}{m}\right)\sin\left(\frac{(k+1)\pi}{m}\right) + \sum_{k=1}^{m-1} \sin\left(\frac{k\pi}{m}\right)^2 \cdot \sum_{k=1}^{n-2} \sin\left(\frac{k\pi}{n}\right)\sin\left(\frac{(k+1)\pi}{n}\right).$$

  – *When m and n are both odd,*

$$Area_T(M) = Area_{VT}(M) = \frac{\sin\left(\frac{\pi}{m}\right)^2 \sin\left(\frac{\pi}{n}\right)^2 \cos\left(\frac{\pi}{\min(m,n)}\right)}{A}.$$

– *When m is odd, n is even, or n is odd, m is even,*

$$Area_T(M) = \frac{\sin\left(\frac{\pi}{m}\right)^2 \sin\left(\frac{\pi}{n}\right)^2 \cos\left(\frac{\pi}{\min(m,n)}\right)}{A}, \quad Area_{VT}(M) = \frac{\sin\left(\frac{\pi}{m}\right)^2 \sin\left(\frac{\pi}{n}\right)^2}{2A}.$$

– *When m and n both even,*

$$Area_T(M) = Area_{VT} = \frac{2\sin\left(\frac{\pi}{m}\right)^2 \sin\left(\frac{\pi}{n}\right)^2 \cos\left(\frac{\pi}{\min(m,n)}\right)}{A}.$$

The formulas in Theorem 4.1.4 are derived by the eigenfunctions of grid graphs in [27].

Theorem 4.1.5. *The three lattice surfaces in [53] and [29] have the following $Area_T$ and $Area_{VT}$:*

- *The lattice surface obtained from the triangle with angles $(\pi/4, \pi/3, 5\pi/12)$ has $Area_T = 1/8 - \sqrt{3}/24 \approx 0.0528312$, $Area_{VT} = \sqrt{3}/6 - 1/4 \approx 0.0386751$.*
- *The lattice surface obtained from the triangle with angles $(2\pi/9, \pi/3, 4\pi/9)$ has $Area_T \approx 0.0259951$, $Area_{VT} \approx 0.0169671$.*
- *The lattice surface obtained from the triangle with angles $(\pi/5, \pi/3, 7\pi/15)$ has $Area_T = Area_{VT} \approx 0.014189$.*

The values of $Area_T$ and $Area_{VT}$ in Theorem 4.1.5 are calculated from the eigenvectors corresponding to the leading eigenvalues of graphs $\mathcal{E}_6$, $\mathcal{E}_7$ and $\mathcal{E}_8$.

4.2 The Calculation of $Area_T$ and $Area_{VT}$

We begin by proving Theorem 4.1.2.

Proof of Theorem 4.1.2. Veech surfaces in the stratum $\mathcal{H}(2)$ have been described completely by Calta [8] and McMullen [39]. Each of them is associated with an order with a discriminant $D \in \mathbb{Z}$, $D > 4$, $D \equiv 0$ or $1 \mod 4$. There are two Teichmüller curves in $\mathcal{H}(2)$ with discriminant D when $D \equiv 1 \mod 8$. There is only one Teichmüller curve in $\mathcal{H}(2)$ with discriminant D otherwise.

When D is a square, the lattice surfaces in $\mathcal{H}(2)$ with discriminant D are square-tiled surfaces, so $Area_T \geq \frac{1}{2\sqrt{D}}$, and $Area_{VT} \geq \frac{1}{2\sqrt{D}}$. On the other hand, Corollary A2 in [39], which gives a description of a pair of cylinder decompositions of such surfaces, shows that $Area_T \leq \frac{1}{2\sqrt{D}}$, and $Area_{VT} \leq \frac{1}{2\sqrt{D}}$. Hence, when D is a square, $Area_T = Area_{VT} = \frac{1}{2\sqrt{D}}$.

Now we consider the case when D is not a square. Consider an embedded triangle on this lattice surface formed by saddle connections. The Veech Dichotomy [52] says that the geodesic flow on a lattice surface is either minimal or completely periodic. Hence, any edge of this triangle must lie on a direction where M can be decomposed into 2 cylinders $M = E_1 \cup E_2$, as shown in Figure 4.3, where the peri-

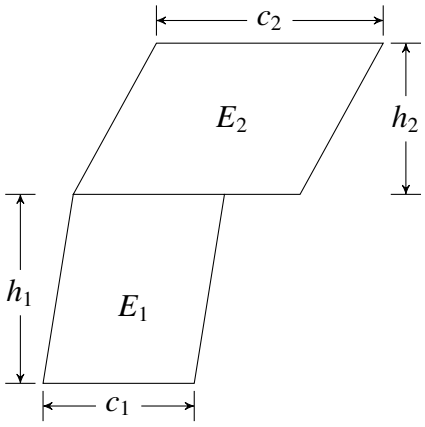

Figure 4.3: A splitting into two cylinders

odic direction is drawn to be the horizontal direction.

Proposition 4.2.1. *Given a 2-cylinder splitting, let as c_1, c_2 and h_1, h_2 be the circumferences and heights of the two cylinders, choose the labels such that $c_1 < c_2$. Then, $Area_T = \min\left\{\frac{c_1h_1}{2}, \frac{c_1h_2}{2}\right\}$, where the minimum is over all possible splittings.*

Proof. For each splitting shown in Figure 4.4, $\frac{c_1h_1}{2}$, $\frac{c_1h_2}{2}$ are the areas of triangle I and triangle II respectively.

Given any embedded triangle formed by saddle connections, split the surface in the direction of one of the sides of this triangle, denoted by a. Choose a as the base, then the height of the triangle with regard to a can not be smaller than the height of the cylinder(s) bordering a. Hence, if the splitting is as shown in Figure 4.4, the area of this triangle can not be smaller than the minimum of the

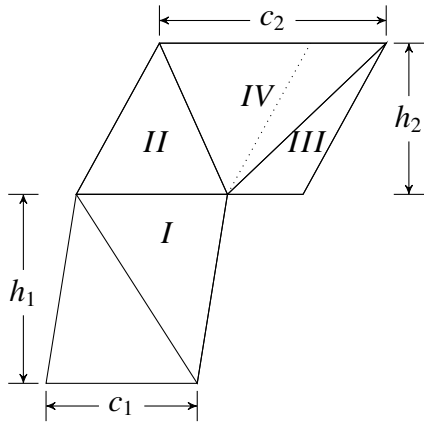

Figure 4.4: The possible triangles.

areas of triangles I, II, III and IV. The area of triangle IV is strictly larger than triangle II because it has the same height and a longer base. Furthermore, after a re-splitting of the surface along the dotted line, the part to the right of the dotted line and the part to the left of the dotted line form two cylinders E_1' and E_2'. We can see that the area of triangle III would be half of the area of E_2', in other words, triangle III has area $\frac{c_1' h_1'}{2}$, where c_i' and h_i' are the circumferences and heights of the cylinders in the new splitting. □

According to Theorem 3.3 of [39], after a $GL(2,\mathbb{R})$ action, we can make any splitting into one of the finitely many prototypes. Each of these prototypes corresponds to an integer tuple (a,b,c,e), and is illustrated in Figure 4.5. Here $\lambda^2 = e\lambda + d$, $bc = d$, $a,b,c \in \mathbb{Z}$, $D = 4d + e^2$.

Define the number e_D as the greatest integer that is both smaller than $\sqrt{D}$ and

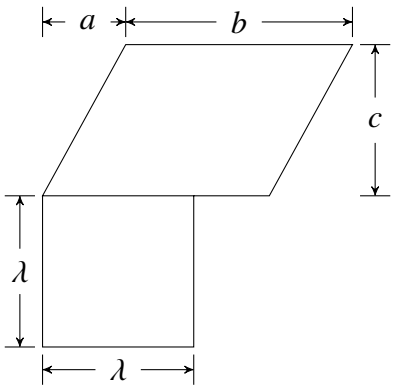

Figure 4.5: Prototypes in $\mathcal{H}(2)$.

congruent to D mod 2. Hence $\sqrt{D} - e_D \leq 2$. So,

$$\min_{M \in E_D \cap \mathcal{H}(2)} Area_T(M) = \inf_{\lambda} \left(\frac{\lambda^2}{2(d+\lambda^2)}, \frac{\lambda}{2(d+\lambda^2)} \right) = \min \left(\frac{1}{2\sqrt{D}}, \frac{\sqrt{D} - e_D}{4\sqrt{D}} \right) = \frac{\sqrt{D} - e_D}{4\sqrt{D}}.$$

Furthermore, when $D \equiv 1 \mod 8$, $(a, b, c, e) = \left(0, \frac{D-e_D^2}{4}, 1, -e_D\right)$ and $(a, b, c, e) = \left(0, 1, \frac{D-e_D^2}{4}, -e_D\right)$ are prototypes of lattice surfaces that are not affinely equivalent, according to Theorem 5.3 in [39]. The areas of red triangles corresponding to these two prototypes dividing by the total area of these surfaces are both $\frac{\sqrt{D}-e_D}{4\sqrt{D}}$, hence surfaces belonging to both components in $E_D \cap \mathcal{H}(2)$ have the same $Area_T$. Hence, $Area_T(M) = \frac{\sqrt{D}-e_D}{4\sqrt{D}}$ for all non-square D and all $M \in E_D \cap \mathcal{H}(2)$.

Now consider $Area_{VT}$. Split the surface in the direction of one of the saddle connections as in Figure 4.3, then the other saddle connection has to cross through either E_1 or E_2. So, the length of their cross product has to be larger than $\min\{c_1, c_2 -$

$c_1\}\min\{h_1, h_2\} = \min\{c_1h_2, h_2(c_2 - c_1), c_1h_1, h_1(c_2 - c_1)\}$. On the other hand, c_1h_2, $h_2(c_2 - c_2)$, and a_1b_1 are twice the areas of the blue, green, and red triangles respectively, so

$$Area_{VT} = \min\left(Area_T, \min\left\{\frac{a_2(b_1 - b_2)}{2Area(M)}\right\}\right).$$

The second minimum goes through all 2-cylinder splittings, or equivalently, all splitting prototypes. Hence,

$$\min\left\{\frac{a_2(b_1 - b_2)}{2Area(M)}\right\} = \min_{prototype} \frac{(b - \lambda)\lambda}{2(d + \lambda^2)} = \min_{prototype} \frac{2b - e - \sqrt{D}}{4\sqrt{D}}.$$

Because $2b - e \equiv D \mod 2$,

$$\frac{2b - e - \sqrt{D}}{4\sqrt{D}} \geq \frac{2 + e_D - \sqrt{D}}{4\sqrt{D}}.$$

On the other hand, the prototype $(a, b, c, e) = \left(0, 1, \frac{D - e_D^2}{4}, -e_D\right)$ satisfies

$$\frac{2b - e - \sqrt{D}}{2\sqrt{D}} = \frac{2 + e_D - \sqrt{D}}{2\sqrt{D}}.$$

So,

$$\min_{M \in E_D \cap \mathcal{H}(2)} Area_{VT}(M) = \min\left(S_V(M), \frac{2 + e_D - \sqrt{D}}{4\sqrt{D}}\right).$$

Therefore, when $D \not\equiv 1 \mod 8$, $Area_{VT}(M) = \min\left(\frac{\sqrt{D} - e_D}{4\sqrt{D}}, \frac{2 + e_D - \sqrt{D}}{4\sqrt{D}}\right)$.

When $D \equiv 1 \mod 8$, the prototypes $(a, b, c, e) = \left(0, e_D + 1 - \frac{D - e_D^2}{4}, \frac{D - e_D^2}{4}, e_D - \frac{D - e_D^2}{2}\right)$ and $(a, b, c, e) = \left(1, e_D + 1 - \frac{D - e_D^2}{4}, \frac{D - e_D^2}{4}, e_D - \frac{D - e_D^2}{2}\right)$ lie on different Teichmüller curves, and both of them satisfy $\frac{2b - e - \sqrt{D}}{2\sqrt{D}} = \frac{2 + e_D - \sqrt{D}}{2\sqrt{D}}$. Hence, both components have the same $Area_{VT}$. In conclusion, $Area_{VT}(M) = \min\left(\frac{\sqrt{D} - e_D}{4\sqrt{D}}, \frac{2 + e_D - \sqrt{D}}{4\sqrt{D}}\right)$ for all $M \in E_D \cap \mathcal{H}(2)$. □

The proofs of Theorem 4.1.3-4.1.5 are similar. Suppose a triangle in a lattice surface has the smallest area. By Veech dichotomy we can decompose the surface into cylinders in the direction of an edge e, then the other edge e' can not cross more than one of such cylinders. Up to Dehn twists along those cylinders (which would not change the cross product $e \times e'$) there are only finitely pairs for each cylinder decomposition. Enumerating all possible types ("prototypes" in the proof of Theorem 4.1.2) of cylinder decompositions up to affine diffeomorphism; then for each of these prototype, enumerate all pairs of saddle connections such that one is in the direction of the circumference, the other crosses one of the cylinders, and that they are two edges of an embedded triangle, then $Area_T$ is the minimal of the areas of those embedded triangles. To simplify the result, we use various geometric and arithmetic considerations as in the proof of Theorem 1.2 to eliminate all but a few cases.

To calculate $Area_{VT}$, do as above while do not require the pair of saddle connections to be two edges of a triangle.

For Theorem 4.1.3 the necessary prototypes of cylinder decompositions are described in section 4 of [30]. They are parametrized by a 5-tuple $(w, h, t, e, \epsilon) \in \mathbb{Z}^5$. Here $\epsilon = \pm 1$ is used to distinguish different types of cylinder configurations. For example, when $\epsilon = 1$, $h > 0$, $0 \leq t < \gcd(w, h)$, $\gcd(w, h, t, e) = 1$, $D = e^2 + 8wh$, $w > \frac{e+\sqrt{D}}{2} > 0$, let $\lambda = \frac{e+\sqrt{D}}{2}$, then the prototype is as shown in Figure 4.6.

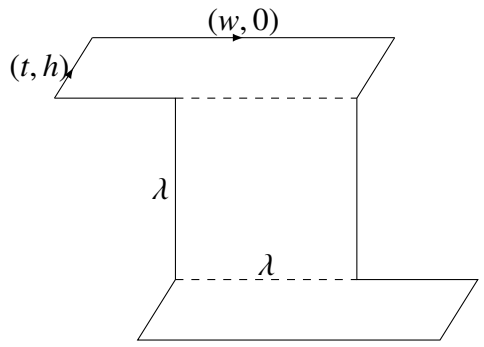

Figure 4.6: Prototypes in $\mathcal{H}(4)$.

For Theorem 4.1.4, the case of regular n-gon can be reduced to a spacial case of the Bouw-Möller surfaces. For Bouw-Möller surfaces, by [55] their $SL(2,\mathbb{R})$ orbits have only two cusps when both m and n are even and only one cusp when otherwise. The $(m-1)\times(n-1)$ grid graphs in [27] gives a Thurston-Veech structure of Bouw-Möller surfaces, whose horizontal and vertical saddle connections are the different when both m and n are even and the same when otherwise. Hence, they provide all the possible cylinder decompositions up to affine action.

The $(m-1)\times(n-1)$ grid graph [27] $G_{m-1,n-1}$ is a ribbon graph that has $(m-1)\times(n-1)$ vertices arranged in $m-1$ rows and $n-1$ columns, each representing a horizontal or vertical cylinder. Up to an affine action, we can make the width of the i,j-th cylinder to be $\sin(i\pi/m)\sin(j\pi/n)$. Then A in the statement of Theorem 4.1.4 is the total area of this surface, $Area_T$ is obtained by finding the smallest rectangle obtained by the intersection of those cylinders, and $Area_{VT}$ is obtained by calculating

the product of the shortest saddle connection in either horizontal or vertical direction and the minimal width of a cylinder in this direction. In the case when both m and n are even, the surface constructed by the grid graph is a double cover of the Bouw-Möller surface, hence the factor of 2 in this case.

For Theorem 4.1.5, in either of the 3 cases, a pair of cylinder decompositions has been described in [32] by one of the three graphs $\mathcal{E}_6$, $\mathcal{E}_7$ or $\mathcal{E}_8$. The horizontal and vertical cylinder decompositions are different, and since the Veech group is a triangle group and the $SL(2,\mathbb{R})$ orbit has only 2 cusps, these two cylinder decomposition types are the only possible ones.

4.3 An enumeration of lattice surfaces with $Area_{VT} > 0.05$

Now we prove Theorem 4.1.1 using the algorithm in [49], which provides a way to list all lattice surfaces and calculate their Veech groups. The algorithm is based on analyzing all Thurston-Veech structures consisting of less than a given number of rectangles.

Let M be a lattice surface. After an affine transformation, we can let the two saddle connections that form the smallest virtual triangle be in the horizontal and

the vertical directions without loss of generality. The Thurston-Veech construction [51] gives a decomposition of M into rectangles using horizontal and vertical saddle connections. The surface M is, up to scaling, completely determined by the configuration of those rectangles as well as the ratios of moduli of horizontal and vertical cylinders. Hence, we can find all lattice surfaces with given $Area_{VT}$ by analyzing all possible Thurston-Veech structures.

Smillie and Weiss presented their algorithm in the following way:

1. Fix $\epsilon > 0$, find all possible pairs of cylinder decompositions with less than $\left\lfloor \frac{1}{2\epsilon} \right\rfloor$ rectangles (there are finitely many such pairs), calculate their intersection matrices and decide the position of cone points.
2. For any number k, find all possible Dehn twist vectors for a k-cylinder decomposition.
3. Use the result from Step (1) and (2) to determine the shape of all possible flat surfaces, and rule out most of them with criteria based on [49], which we will state explicitly later.
4. Rule out the remaining surfaces by explicitly finding pairs of saddle connections with holonomy vectors l, l' such that $\frac{\|l \times l'\|}{2Area(M)} < \epsilon$.

In step (2) and (3), we made some modification to improve the efficiency, which

we will describe below.

Now we describe these steps in greater detail.

Step 1: Choose $\epsilon = 0.05$, find all possible pairs of cylinder decompositions with less than $\left\lfloor \frac{1}{2\epsilon} \right\rfloor = 10$ rectangles. Calculate their intersection matrices and decide the position of cone points.

A pair of cylinder decompositions partition the surface into finitely many rectangles. Let r be the permutation of those rectangles that send each rectangle to the one to its right, and r' be the permutation that send each rectangle to the one below, then the cylinder intersection pattern can be described by these two permutations. According to [49], if M is a lattice surface with $Area_{VT} = \epsilon$, the pair of cylinder decomposition described as above have to decompose the surface into fewer than $\frac{1}{2\epsilon}$ rectangles. Therefore, in this step, we only need to find all transitive pairs of permutations of 9 or less elements up to conjugacy. Furthermore, we do not need to consider those pairs that correspond to a surface of genus 2 or lower, because lattice surfaces of genus 2 or lower have already been fully classified. We also disregard those with one-cylinder decomposition in either the horizontal or vertical direction, because in either case the surface is square-tiled. In order to speed up the conjugacy check of pairs of permutations, we firstly computed the conjugacy classes of all permutations of less than 10 elements and put them in a

look-up table. Then, whenever we need to check if r_1, r_1' and r_2, r_2' are conjugate, we can first check if r_1 and r_1', as well as r_2 and r_2', belong to the same conjugacy classes.

Next, we calculate the following data for these cylinder decomposition: (1) the intersection matrix A; (2) three matrices V, H, D, with entries either 0 or 1, defined as follows:

- $V(i, j) = 1$ iff the i-th horizontal cylinder intersects with the j-th vertical cylinder, and in their intersection there is at least one rectangle such that its upper-left and lower-left corners, or upper-right and lower-right corners are cone points;
- $H(i, j) = 1$ iff the i-th horizontal cylinder intersects with the j-th vertical cylinder, and in their intersection there is at least one rectangle such that its upper-left and upper-right corners, or lower-left and lower-right corners are both cone points;
- $D(i, j) = 1$ iff the i-th horizontal cylinder intersects with the j-th vertical cylinder, and in their intersection there is at least one rectangle such that its lower-right one and the upper-left corners are both cone points.

The matrices V, H, D will be used in the criteria in step 3. To decide whether or not the lower-right corner of the i-th rectangle is a cone point, we calculate $r'r(i)$ and

$rr'(i)$ and check if they are different.

Step 2: For any number k, find all possible Dehn twist vectors for a k-cylinder decomposition.

Equation (9) in the proof of Proposition 3.6 of [49] shows that, if the ratio between the i-th and the j-th entries of a Dehn twist vector is p/q, where p, q are natural numbers and $\gcd(p,q) = 1$, then $pq \leq A_iA_j/\beta^2$, where β is a lower bound of $Area_{VT}$, and A_i is the area of the i-th cylinder divided by the total area. On the other hand, by Cauchy-Schwarz inequality,

$$\begin{aligned}\sum_{i\neq j} A_iA_j =& \frac{1}{2}\left(\left(\sum_i A_i\right)^2 - \sum_i A_i^2\right)\\ =& \frac{1}{2}\left(1 - \sum_i A_i^2\right) \leq \frac{1}{2}\left(1 - \frac{1}{k}\left(\sum_i A_i\right)^2\right)\\ =& \frac{k-1}{2k}.\end{aligned}$$

Hence, we have:

Proposition 4.3.1. *The vector $(n_1, \ldots, n_k)$ cannot be a Dehn twist vector for a surface with $Area_{VT} < \beta$ if $\sum_{1\leq i<j\leq k} s_{ij} \leq \frac{k-1}{2k\beta^2}$, where $s_{ij} = n_in_j/\gcd(n_i,n_j)^2$.*

□

Step 3: Determine the shape of possible surfaces, rule out most of those with

area of virtual triangle smaller than $\epsilon = 0.05$.

For each tuple (A, V, H, D) obtained in step 1, and each Dehn twist vector obtained in step 2, we can calculate the widths and circumferences of cylinders by finding Peron-Frobenious eigenvector as in [51]. Then, we normalize the total area to 1 and check them against the following criteria:

1. Let w_i and w'_j be the widths of the i-th and j-th cylinder in the horizontal and the vertical directions, then $w_i w'_j > 1/10$. This follows from the proof of Proposition 5.1 in [49].
2. Let c_i and c'_j be the circumference of the i-th and j-th cylinder in the horizontal and vertical direction respectively. If the ratio between the moduli of the i-th horizontal cylinder and the i'-th horizontal cylinder is p/q, where p, q are coprime integers, then $c_i w_{i'}/q > 1/10$. This follows from the proof of Proposition 3.5.
3. With the same notation as above, if there are two cone points on the boundary of i-th horizontal cylinder with distance w'_j, and w'_j is not $k_0 c_i/q$ for some integer k_0, then for any integer k, $\max(|w'_j - kc_j/q|, (c_i/q - |w'_j - kc_i/q|)/2)w_{i'} > 1/10$. This is due to an argument similar to the proof of Proposition 3.5 as follows: after a suitable parabolic affine action we can assume that there is a vertical saddle connection crossing the i'-th cylinder. Let the holonomy vectors of two saddle connections crossing the i-th cylinder from a same cone

point to those two cone points be $(x + nc_i, w_i)$ and $(x + w'_j + n'c_i, w_i)$, where $n, n' \in \mathbb{Z}$. Do a parabolic affine action on the surface that is a Dehn twist on the i'-th cylinder, then their holonomy vectors will become $(x + rc_i/q + nc_i, w_i)$ and $(x + w'_j + rc_i/q + n'c_j, w_i)$, where $\gcd(r, q) = 1$. Repeatedly doing such affine actions, we can see that the absolute value of horizontal coordinate of the holonomy vector of at least one saddle connection we get is nonzero and no larger than $\max(|w'_j - kc_j/q|, (c_i/q - |w'_j - kc_i/q|)/2)$.

4. Criteria (2) and Criteria (3) apply to vertical, instead of horizontal cylinders.
5. The cross product of the holonomy vectors of diagonal saddle connections from the upper-left corner to the lower-right corner must be either 0 or larger than $1/10$.

In our calculation, we used an optimization which rules out some Dehn twist vectors before the calculation of Peron-Frobenious eigenvector. Firstly, in Step 1, we label the cylinders by the number of rectangles they contain in decreasing order. Then, when we generate Dehn twist vectors, we calculate the product of the last two entries. Now the last two horizontal or vertical cylinders always have the least number of rectangles, and the sum of their areas is less than $(1 - c/10)$ of the total area, where c is the number of rectangles not in these two cylinders. Hence, we can bound the product of their areas which in turn gives an upper bound on the product of the last two elements of the Dehn twist vector. We used the C++ linear algebra library Eigen, and the first 3 steps were done in a few hours.

If a 4-tuple (A, V, H, D) and a pair of Dehn twist vectors pass through all the above-mentioned tests, they are printed out together with the eigenvector (w_i). Below is a sample of the output of this step:

$$A = \begin{pmatrix} 3 & 1 & 1 \\ 1 & 0 & 0 \end{pmatrix}, V = \begin{pmatrix} 1 & 1 & 1 \\ 1 & 0 & 0 \end{pmatrix}, H = \begin{pmatrix} 1 & 0 & 1 \\ 1 & 0 & 0 \end{pmatrix}, D = \begin{pmatrix} 1 & 0 & 1 \\ 1 & 0 & 0 \end{pmatrix}$$

$n = (2, 7), n' = (2, 5, 5), w = (1, 1)$

$$A = \begin{pmatrix} 6 & 1 \\ 1 & 1 \end{pmatrix}, V = \begin{pmatrix} 0 & 0 \\ 0 & 0 \end{pmatrix}, H = \begin{pmatrix} 0 & 0 \\ 0 & 0 \end{pmatrix}, D = \begin{pmatrix} 0 & 0 \\ 0 & 1 \end{pmatrix}$$

$n = (1, 4), n' = (1, 4), w = (1, 1.23607)$

$n = (2, 7), n' = (2, 7), w = (1, 1)$

$$A = \begin{pmatrix} 5 & 2 \\ 1 & 1 \end{pmatrix}, V = \begin{pmatrix} 0 & 0 \\ 0 & 0 \end{pmatrix}, H = \begin{pmatrix} 1 & 0 \\ 0 & 0 \end{pmatrix}, D = \begin{pmatrix} 1 & 0 \\ 0 & 1 \end{pmatrix}$$

$n = (2, 7), n' = (1, 2), w = (1, 1)$

$$A = \begin{pmatrix} 6 & 1 \\ 2 & 0 \end{pmatrix}, V = \begin{pmatrix} 1 & 1 \\ 0 & 0 \end{pmatrix}, H = \begin{pmatrix} 1 & 1 \\ 1 & 0 \end{pmatrix}, D = \begin{pmatrix} 0 & 1 \\ 0 & 0 \end{pmatrix}$$

$n = (1, 4), n' = (1, 16), w = (1, 1)$

$n = (2, 7), n' = (1, 8), w = (1, 1)$

$$A = \begin{pmatrix} 5 & 1 & 1 \\ 1 & 1 & 0 \end{pmatrix}, V = \begin{pmatrix} 1 & 0 & 1 \\ 0 & 0 & 0 \end{pmatrix}, H = \begin{pmatrix} 1 & 0 & 1 \\ 0 & 0 & 0 \end{pmatrix}, D = \begin{pmatrix} 1 & 0 & 1 \\ 0 & 1 & 0 \end{pmatrix}$$

$n = (1, 4), n' = (1, 3, 12), w = (1, 1)$

$n = (2, 7), n' = (1, 3, 6), w = (1, 1)$

Each 4-tuple (A, V, H, D) is followed by pairs of Dehn twist vectors n, n' in the horizontal and vertical directions respectively, and a vector of widths w. This section of the output described 8 combinations of (A, V, H, D) and Dehn twist vectors, only the second one will result in a non-arithmetic surface, while other line all correspond to square-tiled cases, which we verified through integer arithmetic.

After collecting all tuples (A, V, H, D) that may generate non-arithmetic surfaces that pass the test in this step, we can use the same algorithm in step 1 to find all pairs of permutations corresponding to these tuples, hence completely decide the shape of surfaces we need to check in the next step.

Step 4: After the previous 3 steps, we can show that any non square-tiled lattice surface with area of the smallest virtual triangle larger than $1/20$ is either of genus 2, or $GL(2, \mathbb{R})$-equivalent to one of the 50 remaining cases. Two of them are the Prym eigenform of discriminant 8 in genus 3. By finding saddle connections on the remaining 48 surfaces by hand, we showed that none of them has $Area_{VT}$ greater than $1/20$.

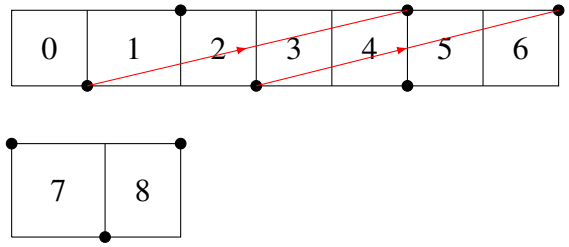

Figure 4.7: Permutations: (in cycle notation) $(0,1,2,3,4,5,6)(7,8)$, $(0,4,6,3,5,2,8)(1,7)$; Dehn twist vectors: $(1,4)$, $(1,4)$. Dots are cone points. The holonomies of the two red saddle connections depicted have a cross product less than 1/10 of the surface area.

An example of one of the 48 surfaces is shown in Figure 4.7.

Below is the list of all the 48 surfaces we checked by hand, none has $Area_{VT} > 1/20$. All surfaces are represented by a pair of permutations (written in cycle notation, the i-th cycle is the i-th (horizontal or vertical) cylinder) and two Dehn twist vectors.

1. Dehn twist vectors: (3,4), (1,2);

   pair of permutations:

   (0,1,2,3,4)(5,6,7,8), (0,3,1,6,5,8)(4,2,7)

2. Dehn twist vectors: (1,4), (1,4);

   pairs of permutations:

   (0,1,2,3,4,5,6)(7,8), (0,3,4,5,6,2,8)(1,7)

(0,1,2,3,4,5,6)(7,8), (0,4,3,5,6,2,8)(1,7)

(0,1,2,3,4,5,6)(7,8), (0,5,3,4,6,2,8)(1,7)

(0,1,2,3,4,5,6)(7,8), (0,4,5,3,6,2,8)(1,7)

(0,1,2,3,4,5,6)(7,8), (0,3,5,4,6,2,8)(1,7)

(0,1,2,3,4,5,6)(7,8), (0,5,4,3,6,2,8)(1,7)

(0,1,2,3,4,5,6)(7,8), (0,6,3,4,5,2,8)(1,7)

(0,1,2,3,4,5,6)(7,8), (0,4,6,3,5,2,8)(1,7)

(0,1,2,3,4,5,6)(7,8), (0,5,6,3,4,2,8)(1,7)

(0,1,2,3,4,5,6)(7,8), (0,4,5,6,3,2,8)(1,7)

(0,1,2,3,4,5,6)(7,8), (0,6,3,5,4,2,8)(1,7)

(0,1,2,3,4,5,6)(7,8), (0,5,4,6,3,2,8)(1,7)

(0,1,2,3,4,5,6)(7,8), (0,3,6,4,5,2,8)(1,7)

(0,1,2,3,4,5,6)(7,8), (0,6,4,3,5,2,8)(1,7)

(0,1,2,3,4,5,6)(7,8), (0,5,3,6,4,2,8)(1,7)

(0,1,2,3,4,5,6)(7,8), (0,6,4,5,3,2,8)(1,7)

(0,1,2,3,4,5,6)(7,8), (0,3,5,6,4,2,8)(1,7)

(0,1,2,3,4,5,6)(7,8), (0,5,6,4,3,2,8)(1,7)

(0,1,2,3,4,5,6)(7,8), (0,3,5,6,4,2,8)(1,7)

(0,1,2,3,4,5,6)(7,8), (0,3,4,6,5,2,8)(1,7)

(0,1,2,3,4,5,6)(7,8), (0,4,3,6,5,2,8)(1,7)

(0,1,2,3,4,5,6)(7,8), (0,6,5,3,4,2,8)(1,7)

(0,1,2,3,4,5,6)(7,8), (0,4,6,5,3,2,8)(1,7)

(0,1,2,3,4,5,6)(7,8), (0,3,6,5,4,2,8)(1,7)

3. Dehn twist vectors: (1,2), (1,3);

   pairs of permutations:

   (0,1,2,3,4)(5,6,7), (0,5,1,6,2,7)(3,4)

   (0,1,2,3,4)(5,6,7), (1,4,6,2,3,5)(0,7)

4. Dehn twist vectors: (1,2), (1,2);

   pairs of permutations:

   (0,1,2,3,4)(5,6,7), (0,2,4,6,7)(1,3,5)

   (0,1,2,3,4)(5,6,7), (0,4,3,6,7)(1,2,5)

   (0,1,2,3,4)(5,6,7), (0,5,2,3,7)(1,3,6)

   (0,1,2,3,4)(5,6,7), (1,3,6,2,5)(0,4,7)

   (0,1,2,3,4)(5,6,7), (0,5,1,4,7)(2,3,6)

   (0,1,2,3,4)(5,6,7), (0,6,2,3,7)(1,4,5)

   (0,1,2,3,4)(5,6,7), (0,5,1,3,7)(2,4,6)

   (0,1,2,3,4)(5,6,7), (0,4,6,2,7)(1,3,5)

   (0,1,2,3,5)(5,6,7), (0,6,3,2,7)(1,4,5)

5. Dehn twist vectors: (1,2), (1,1);

   pair of permutations:

   (0,1,2,3,4)(5,6,7), (0,3,6,7)(1,4,2,5)

6. Dehn twist vectors: (2,7), (2,7);

   pair of permutations:

   (0,1,2,3,4,5)(6,7), (0,3,4,5,2,7),(1,6)

7. Dehn twist vectors: (1,1), (1,1);

   pair of permutations:

(0,1,2,3)(4,5,6), (0,3,5,6)(1,2,4)

8. Dehn twist vectors: (1,2), (1,2);

   pairs of permutations:

   (0,1,2,3)(4,5,6), (0,3,5,6)(1,2,4)

   (0,1,2,3)(4,5,6), (0,2,4,6)(1,3,5)

   (0,1,2,3)(4,5,6), (1,4,2,5)(0,3,6)

   (0,1,2,3)(4,5,6), (1,5,2,4)(0,3,6)

   (0,1,2,3)(4,5,6), (0,2,4,6)(1,5,3)

   (0,1,2,3)(4,5,6), (0,1,4,6)(2,5,3)

9. Dehn twist vectors: (1,3), (1,3);

   pairs of permutations:

   (0,1,2,3,4)(5,6), (0,3,4,2,6)(1,5)

10. Dehn twist vectors: (1,3), (1,3);

    pairs of permutations:

    (0,1,2,3)(4,5), (0,2,3,5)(1,4)

    (0,1,2,3)(4,5), (0,1,3,5)(2,4)

And the two lattice surfaces that are Prym eigenforms in genus 3 are as follows:

- Dehn twist vectors (1,1,1), (1,1,1);

  pairs of permutations:

  (0,1,2)(3,4)(5,6), (0,4,6)(1,5)(2,3)

  (0,1,2)(3,4)(5,6), (1,4,5)(0,6)(2,3).

CHAPTER 5

ABELIAN COVERS OF THE FLAT PILLOWCASE

5.1 Introduction

The flat pillowcase has a half translation structure, which induces a half-translation structure on its branched covers. In this chapter, we give a comprehensive treatment of the relative cohomology of branched abelian normal covers of the flat pillowcase, the action of the affine diffeomorphism group of these branched cover on their relative cohomology, as well as invariant subspaces under this group action. These subspaces are orthogonal under an invariant Hermitian norm. The corresponding question for absolute cohomology is a classical one related to the monodromy of the hypergeometric functions which dates back to Euler and is outlined in [12] (see also [55]). Most previous work on this topic focuses on the case of absolute cohomology, and uses holomorphic methods. Due to the recent interest in translation surfaces and $SL(2,\mathbb{R})$-orbit closures in them, there is also interest in the relative cohomology $H^1(M,\Sigma;\mathbb{C})$ because the relative cohomology is the tangent space of strata, and because these branched covers are in $SL(2,\mathbb{R})$ closed orbits. For example, Matheus and Yoccoz [37] calculate the action of the full affine group on the relative cohomology of two well-known translation surfaces, the Wollmilchsau and the Ornithorynque, both of which are examples of abelian branched covers of the flat pillowcase. In this chapter, we will give a complete description of the action of the full affine group on relative cohomology

of all abelian branched covers of the pillowcase.

We will begin by showing that there is a direct sum decomposition of the relative cohomology, and calculate the dimension of the summands.

Theorem 5.1.1. *Let M be a branched cover of the pillowcase with deck group G. Let $\Sigma \subset M$ be the preimage of the four cone points of the pillowcase. Let Δ be the set of irreducible representations of a finite abelian group G. These are all one dimensional, hence are homomorphisms from G to $\mathbb{C}^*$. Deck transformations give an action of G on $H^1(M, \Sigma; \mathbb{C})$. Let $H^1(\rho)$ be the sum of G-submodules of $H^1(M, \Sigma; \mathbb{C})$ isomorphic to ρ.*

1. $$H^1(M, \Sigma; \mathbb{C}) = \bigoplus_{\rho \in \Delta} H^1(\rho)$$
   this decomposition is preserved by the action of the affine group **Aff**, *while the factors may be permuted.*
2. *The dimension of $H^1(\rho)$ is 3 if ρ is the trivial representation and 2 otherwise.*

The space $H^1(\rho)$ can also be described as cohomology of the pillowcase with twisted coefficients as in [12], [50]. Let $H^1_{abs}(\rho)$ be the sum of G-submodules of $H^1(M; \mathbb{C})$ isomorphic to ρ, then there is also a splitting $H^1(M) = \bigoplus_\rho H^1_{abs}(\rho)$ which was described in [55].

There is a natural projection $r : H^1(M, \Sigma; \mathbb{C}) \to H^1(M; \mathbb{C})$ induced by the inclusion $(M, \emptyset) \to (M, \Sigma)$, which is also equivariant under the deck group G. The kernel of r is called the *rel*-space. It is interesting to know when this projection splits equivariantly, in other words, when *rel* has an **Aff**-invariant complement.

Because r is G-equivariant and surjective, it sends $H^1(\rho)$ surjectively to $H^1_{abs}(\rho)$. For abelian branched covers of the pillowcase, we can describe r by describing its restriction to each $H^1(\rho)$. The result can be summarized as follows:

Theorem 5.1.2. *Let M, Σ, r be as above, let g_i, $i = 1, 2, 3, 4$ be the elements in deck group G that correspond to the counterclockwise loops around the 4 cone points of the pillowcase, then:*

1. *If two or four of the four $\rho(g_j)$ are equal to 1 then $r|_{H^1(\rho)} = 0$, hence $H^1_{abs}(\rho) = 0$.*
2. *If only one of the four $\rho(g_j)$ is 1 then $\ker(r|_{H^1(\rho)}) \to H^1(\rho) \to r(H^1(\rho))$ does not split as a Γ-module. In this case $H^1_{abs}(\rho)$ has dimension 1.*
3. *In all other cases, $r|_{H^1(\rho)}$ is bijective hence splits. In this case $H^1_{abs}(\rho)$ has dimension 2.*

In summary, $r : H^1(M, \Sigma; \mathbb{C}) \to H^1(M; \mathbb{C})$ splits if and only if case (2) does not appears, i.e. if and only if for any $i \in \{1, 2, 3, 4\}$, either the subgroup generated by g_i, (g_i), contains g_j for some $j \neq i$, or $G/(g_i) = (\mathbb{Z}/2)^2$.

For example, when M is the Wollmilchsau, r splits, because $(g_1) = (g_2) = (g_3) =$

$(g_4) = G$ [37].

The dimension of $H^1_{abs}(\rho)$ was calculated in [55].

There is a natural invariant Hermitian form on $H^1(M, \Sigma; \mathbb{C})$ (see [12], [50] or Section 5.4). In case (1) this form is trivial, in case (2) this form induces an Euclidean structure on its complex projectivization $\mathbb{P}(H^1(\rho))$, and in case (3) it may be positive definite, negative definite or indefinite, depending on the arguments of $\rho(g_i)$, hence induces either a spherical or hyperbolic structure on $\mathbb{P}(H^1(\rho))$. The relation between the signature of this Hermitian form on $H^1(\rho)$ and the arguments of $\rho(g_i)$ was given in [12] as a consequence of Riemann-Roch, and a more elementary proof is included here as Theorem 5.4.1.

In section 5.5 we will describe a subgroup of finite index Γ_1 of the affine diffeomorphism group. The subspaces $H^1(\rho)$ are invariant under Γ_1 and the action of Γ_1 can be described as follows:

Theorem 5.1.3. *If ρ satisfy the conditions in case (2) and (3) of Theorem 1.2, the action of $\Gamma_1 \subset$ **Aff** on $\mathbb{P}H^1(\rho) = \mathbb{CP}^1$ factors through an index-2 subgroup of a (Euclidean, hyperbolic or spherical) triangle group.*

By considering the angles of the corresponding triangle, we can easily deter-

mine when Γ_1, hence the **Aff**, acts discretely on $H^1(\rho)$.

As an application of these results, we will construct examples of translation surfaces, which answer a question of Smillie and Weiss. In [47], they use these examples to show that horocycle orbit closures in strata may be non-affine. For their examples, Smillie and Weiss require that there is an invariant subspace of $H^1(M, \Sigma; \mathbb{C})$ defined over $\mathbb{R}$. Define complex conjugation in $H^1(M, \Sigma; \mathbb{C})$ by the complex conjugate in coefficient field $\mathbb{C}$. For any subspace $N \subset H^1(M, \Sigma; \mathbb{C})$, let $\overline{N}$ be the complex conjugate of N. A complex subspace N is defined over $\mathbb{R}$ i.e. $N = Re(N) \otimes \mathbb{C}$, if and only if $\overline{N} = N$.

Proposition 5.1.4. *There is a square-tiled surface M on which all points in Σ are singular, constructed as a normal abelian branched cover of the flat pillowcase such that:*

1. *there is a direct sum decomposition $H^1(M, \Sigma; \mathbb{C}) = N \oplus \overline{N} \oplus H$ preserved by the action of the group of orientation preserving affine diffeomorphisms. Furthermore, H is defined over $\mathbb{R}$.*
2. *there is a positive or negative definite Hermitian norm on N invariant under the affine diffeomorphism group action*
3. *the affine diffeomorphism group action on N does not factor through a discrete group.*

Remark 5.1.1. The decomposition $H^1(M, \Sigma; \mathbb{C}) = N \oplus \overline{N} \oplus H$ implies that $H^1(M, \Sigma; \mathbb{R}) = Re(N) \oplus Re(H)$. Furthermore, N, $\overline{N}$ and H are orthogonal to each other with respect

to the invariant Hermitian form, and the tangent space of the $GL(2,\mathbb{R})$ orbit of M lies in H

Hubert-Schmithüsen [28] gave a proof of the non-discreteness of the action of the affine group in some cases using Lyapunov exponents and Galois conjugation. Forni-Matheus-Zorich [22], Bouw-Möller [6], Deligne-Mostow [12], Thurston [50], Alex Wright [55], McMullen [38] and Eskin-Kontsevich-Zorich [14] calculated the action on cohomology and provided discreteness criteria under different contexts.

We will give a description of the affine diffeomorphism group of these surfaces in Section 5.2, and define the group Γ. In Section 5.3, we will prove Theorem 5.1.1. In Section 5.4, we define and calculated the signature of an invariant Hermitian form. In Section 5.5 we will define Γ_1 and prove Theorem 5.1.2 and 5.1.3. In Section 5.6 we will discuss the discreteness criteria and construct examples that establish Proposition 5.1.4. As pointed out by Alex Wright, the existence of examples answering the question of Smillie and Weiss follows from the following ingredients: firstly, Theorem 5.1.1, secondly, a signature calculation of the Hodge form on each component, and thirdly, a discreteness criteria. The discreteness criteria and signature calculation in [12], together with Theorem 5.1.1, are already enough for the construction of many such examples.

We will now set up some notation to describe normal branched covers of the pillowcase. Let P be the unit flat pillowcase with four cone points z_1, z_2, z_3 and z_4

of cone angle π. We build P by identifying edges with the same label as in Figure 5.1:

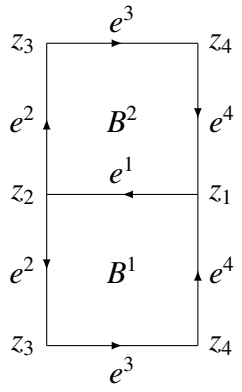

Figure 5.1: A flat pillowcase.

Let G be a finite group and $\mathbf{g} = (g_1, \ldots, g_4) \in G^4$ a 4-tuple of elements in G such that $g_1g_2g_3g_4 = 1$. Let $M = M(G, \mathbf{g})$ be the connected normal branched cover of P branching at $z_1, \ldots z_4$, with deck transformation group G acting on the left. Let l_j be a simple loop around z_j that travels in counter-clockwise direction on P based in B^1. It lifts to a path from the preimage of B^1 in the g-th sheet of the cover to the preimage of B^1 in the gg_j-th sheet. In other words, $\mathbf{g}$ gives a group homomorphism from

$$\pi_1(P - \{z_1, z_2, z_3, z_4\}) = \langle l_1, l_2, l_3, l_4 | l_1l_2l_3l_4 = 1 \rangle$$

to G. Here the homomorphism defined by $\mathbf{g}$ sends the element in $\pi_1(P - \{z_1, z_2, z_3, z_4\})$ represented by l_j to $g_j \in G$. The connectedness of M is equivalent to the condition that $\{g_1, \ldots, g_4\}$ generate G. Let Σ denote the set of preimages of all points z_j, $j = 1, \ldots, 4$. The surface M has a half translation structure induced by

the half translation structure on P.

When the orders of g_j are all even, all the holonomies are translations and M is a translation surface. When the order of g_j is 2, the corresponding vertex has cone angle 2π. When none of the orders of g_j is 2, Σ consists of actual cone points of M, in which case **Aff** is the affine diffeomorphism group.

The decomposition of P into two squares in figure 5.1 induces a cell decomposition on $M(G, \mathbf{g})$, which can be described as $|G|$-copies of pairs of squares labeled by elements in G as B^1_g, B^2_g, that are glued together by identifying edges e^j_g and $e^{j'}_{g'}$ when $j = j'$ and $g = g'$, so that the directions indicated by the arrows match:

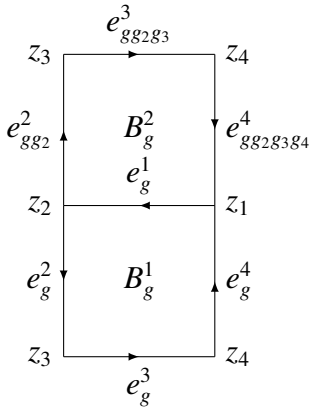

Figure 5.2: A leaf in the branched cover.

For example, in our notation the Wollmilchsau [20, 25] is $M(\mathbb{Z}/4, (1, 1, 1, 1))$, can be presented as the union of the following squares with indicated glueings :

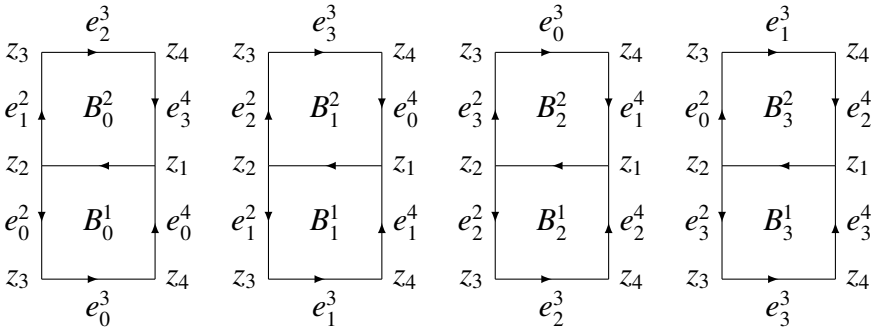

Figure 5.3: Wollmilchsau as a branched cover of the flat pillowcase.

As another example, let $G = \mathbb{Z}/3$ and $\mathbf{g} = (0, 1, 1, 1)$. In this case $M = M(G, \mathbf{g})$ is a half translation surface and the gluing is as follows:

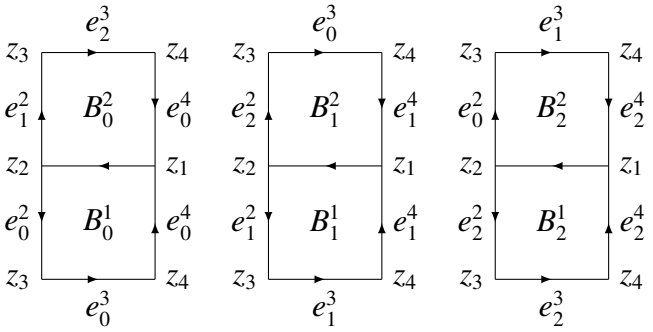

Figure 5.4: $M(\mathbb{Z}/3, (0, 1, 1, 1))$.

Our notation is closely related to but not identical with that used in [55]. In [55], an abelian branched cover of P is described by a positive integer N and a n-by-4 matrix A, and is denoted by $M_N(A)$. In our notation, it becomes $M(span(\mathbf{q}_1, \mathbf{q}_2, \mathbf{q}_3, \mathbf{q}_4)$,
$(\mathbf{q}_1, \mathbf{q}_2, \mathbf{q}_3, \mathbf{q}_4))$, where $\mathbf{q}_j \in (\mathbb{Z}/N)^n$ are the column vectors of A.

Now we describe the action of the deck group G on $M(G, \mathbf{g})$. An element $h \in G$ sends B_g^k to B_{hg}^k and e_g^k, to e_{hg}^k. The deck group action induces a right G-action on $H^1(M, \Sigma; \mathbb{C})$ that makes it a right G-module.

5.2 Affine diffeomorphisms

From now on we assume that G is abelian, though many of our arguments work for any finite group. At the end of this section we will point out the modifications required in the non-Abelian case.

In this section we will calculate $\mathbf{Aff} = \mathbf{Aff}(M(G, \mathbf{g}))$, as well as the Veech group.

Our method is inspired by the coset graph description used in [44]. One distinction between the two approaches is that we consider the whole affine diffeomorphism group while [44] considers the Veech group. Fixing G, let V be the set of all 4-tuples of elements in G: $\mathbf{h} = (h_1, h_2, h_3, h_4)$ such that $\{h_1, h_2, h_3, h_4\}$ generates G and $h_1 h_2 h_3 h_4 = 1$. Each 4-tuple in V is associated with a square-tiled surface $M(G, \mathbf{h})$ which is equipped with a cell decomposition labeled as in figure 5.2. An element F in $\mathbf{Aff}$ induces an automorphism of the deck group G by $g \mapsto FgF^{-1}$, i.e. there is a group homomorphism $\mathbf{Aff} \to Aut(G)$. We denote by Γ the kernel of

this homomorphism. Because $Aut(G)$ is a finite group, Γ is a subgroup of **Aff** with finite index.

We will show that all orientation preserving affine diffeomorphisms between various surfaces $M(G, \mathbf{h})$ with G fixed and $\mathbf{h}$ varying in V, that preserves Σ are compositions of a finite set of affine diffeomorphisms. We call this set the set of basic affine diffeomorphisms, and we will describe them below. In our discussion we will be dealing with both translation surfaces and half translation surfaces. It will be convenient to view the derivative of an affine diffeomorphism as an element of $PGL(2, \mathbb{R}) = GL(2, \mathbb{R})/\{\pm I\}$. We will call an affine translation diffeomorphism a half translation equivalence when its derivative is 1 in $PGL(2, \mathbb{R})$.

Now we define four of the five classes of the basic affine diffeomorphisms:

(i) Rotation: For any $(h_1, h_2, h_3, h_4) \in V$, let $t_{(h_1,h_2,h_3,h_4)}$ be the map from $M(G, (h_2, h_3, h_4, h_1))$ to $M(G, (h_1, h_2, h_3, h_4))$ that sends B^1_e of $M(G, (h_2, h_3, h_4, h_1))$ to B^1_e of $M(G, (h_1, h_2, h_3, h_4))$ by rotating counterclockwise by $\pi/2$.

(ii) Deck transformation: For any $(h_1, h_2, h_3, h_4) \in V$, $g \in G$, let $r_{g,\mathbf{h}}$ be the deck transformation g in $M(G, \mathbf{h})$. Its derivative is the identity.

(iii) Interchange of B^1 and B^2: For any $(h_1, h_2, h_3, h_4) \in V$, let $f_{(h_1,h_2,h_3,h_4)}$ be the map from $M(G, (h_2, h_1, h_1^{-1}h_4h_1, h_2h_3h_2^{-1}))$ to $M(G, (h_1, h_2, h_3, h_4))$ which interchanges B^1_g and B^2_g by a rotation of π.

(iv) Relabeling: For any $(h_1, h_2, h_3, h_4) \in V$, $\psi \in Aut(G)$, let m_ψ be the map from $M(G, \mathbf{h})$ to $M(G, \psi(\mathbf{h}))$ that sends B^j_g to $B^j_{\psi(g)}$. Its derivative is the identity.

We claim that:

Lemma 5.2.1. *Any half translation equivalence from $M(G, \mathbf{h})$ to $M(G, \mathbf{h}')$ can be written as composition of basic affine diffeomorphisms t^2, r, f and m.*

Proof. Let F_0 be such a half translation equivalence. Denote the unit element of G as e. By our assumption, F_0 preserves Σ, hence it is a permutation of unit squares that tiled M and M'. More precisely, F_0 is completely determined by the following data: i) the induced automorphism ψ of deck group, ii) a number $j = 1$ or 2, which is 1 when B^1 and B^2 are taken to themselves and 2 when they are interchanged, an element $g \in G$, such that $F_0(B^1_e) = B^j_g$, and iii) a number s, which is 0 if $F_0^{-1}(e^1_g)$ is e^1_e, 1 if $F_0^{-1}(e^1_g)$ is e^3_e. Hence, $F_0 = m_\psi t^{2s} f^{j-1} r_g$. □

For general orientation preserving affine diffeomorphism F, its derivative DF will be in $PSL(2, \mathbb{Z})$. We add another class of basic affine diffeomorphisms:

(v) Shearing: For any $(h_1, h_2, h_3, h_4) \in V$, let $s_{(h_1,h_2,h_3,h_4)}$ be a map from $M(G, (h_1 h_2 h_1^{-1}, h_1, h_3, h_4))$ to $M(G, (h_1, h_2, h_3, h_4))$ that sends e^3_1 to e^3_1 and has derivative $\begin{pmatrix} 1 & -1 \\ 0 & 1 \end{pmatrix}$.

Because the derivative of s and t generate $PSL(2,\mathbb{Z})$, by successively composing with s and t we can reduce to the case when the derivative is the identity. Hence given any $\mathbf{h}, \mathbf{h}' \in V$, any affine diffeomorphism from $M(G,\mathbf{h})$ to $M(G,\mathbf{h}')$ that sends Σ to Σ, or more specifically, any element in **Aff**, is a composition of the five classes of maps described above. Because m commutes with other 4 classes of diffeomorphisms, i.e.

$$m_\psi t_{\mathbf{h}} = t_{\psi(\mathbf{h})} m_\psi$$

$$m_\psi r_{g,\mathbf{h}} = r_{\psi(g),\psi(\mathbf{h})} m_\psi$$

$$m_\psi f_{\mathbf{h}} = f_{\psi(\mathbf{h})} m_\psi$$

$$m_\psi s_{\mathbf{h}} = s_{\psi(\mathbf{h})} m_\psi$$

any $F \in \mathbf{Aff}$ can be written as $F = F_1 m_\psi$ where F_1 is a composition of t, s, r and f, while ψ is the automorphism of deck group induced by F. Hence, elements in Γ can be written as successive compositions of t, r, f and s.

As in [44], we will define a directed graph D with vertex set V. Each element $\mathbf{h} \in V$ corresponds to a surface $M(G,\mathbf{h})$. An edge in the graph corresponds to a basic affine diffeomorphism between two $M(G,\mathbf{h})$. Paths starting and ending at $M(G,\mathbf{g})$ correspond to elements in **Aff**. Now the fact that any affine diffeomorphism is a successive composition of t, s, r, f, and m means that the map from the set of such paths to **Aff** is surjective. Similarly, let D_0 be graph D with those edges corresponding to m removed, then the set of paths starting and ending at $\mathbf{g}$ in D_0

maps surjectively to Γ.

Consider the example for which $G = \mathbb{Z}/6$ and $\mathbf{g} = (1, 1, 1, 3)$. This example is the Ornithorynque (c.f.[21]). In the following figure we give the connected component of D that contains $\mathbf{g}$, with loops corresponding to deck transformation (i.e. all the r arrows) omitted:

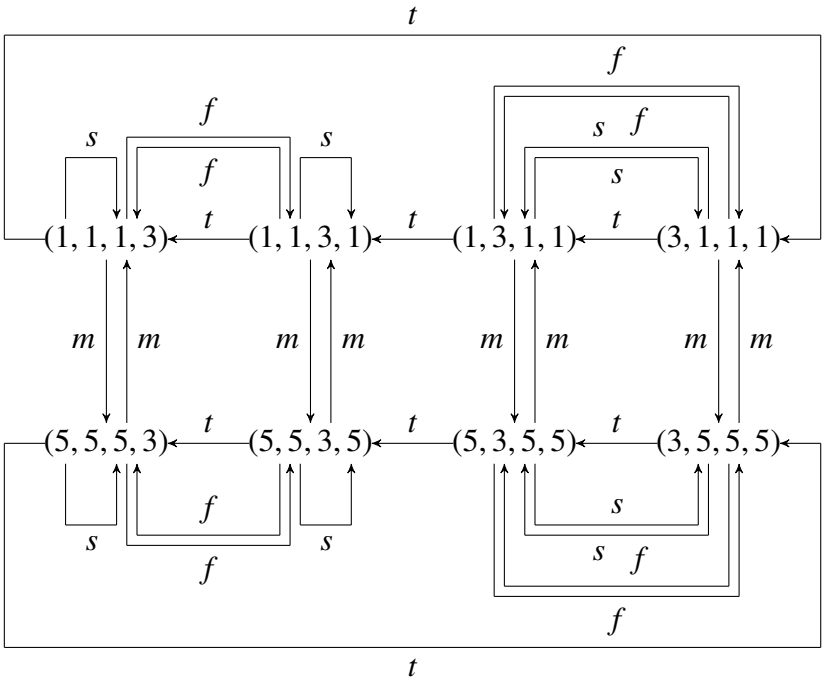

Figure 5.5: Connected component of the graph D for the Ornithorynque, with r arrows removed.

Aff of the Ornithorynque can be calculated by finding loops in D that start and end at $\mathbf{g} = (1, 1, 1, 3)$. In this case, **Aff** is generated by tf, s, and $r_{2,(1,1,1,3)}$.

The Veech group is the subgroup of $SL(2,\mathbb{R})$ generated by the derivative of these generators.

We will show in the next section that the subspaces $H^1(\rho)$ in Theorem 5.1.1 are invariant under Γ.

This method of calculating **Aff** does not use the fact that G is abelian in any way.

5.3 An invariant decomposition of relative cohomology

We will now prove Theorem 5.1.1. Furthermore, we will show that $H^1(\rho)$ are invariant under Γ described in the previous section. The proof below can also be viewed as calculation of cohomology with twisted coefficients of P, c.f. [24]

Proof of Theorem 5.1.1. Let $M = M(G, \mathbf{g})$, $\Sigma \subset M$ as in Section 5.1, consider the relative cellular cochain complex

$$0 \to C^1(M, \Sigma; \mathbb{C}) \to C^2(M, \Sigma; \mathbb{C}).$$

We can identify $C^1(M, \Sigma; \mathbb{C})$ with $(\mathbb{C}[G])^4$ as a right-G module by writing $m \in$

$C^1(M, \Sigma; \mathbb{C})$ as

$$(\sum_g m(e_g^1)g^{-1}, \sum_g m(e_g^2)g^{-1}, \sum_g m(e_g^3)g^{-1}, \sum_g m(e_g^4)g^{-1}) \in (\mathbb{C}[G])^4.$$

We can also identify $C^2(M, \Sigma; \mathbb{C})$ with $(\mathbb{C}[G])^2$ as a right-G module by writing $n \in C^2(M, \Sigma; \mathbb{C})$ as

$$(\sum_g n(B_g^1)g^{-1}, \sum_g n(B_g^2)g^{-1}) \in (\mathbb{C}[G])^2.$$

Then, the coboundary map from C^1 to C^2 becomes

$$d^1(a, b, c, d) = (a + b + c + d, a + g_2 b + g_2 g_3 c + g_2 g_3 g_4 d). \tag{5.1}$$

Hence:

$$H^1(M, \Sigma; \mathbb{C}) = \{(a, b, c, d) \in (\mathbb{C}[G])^4 : a+b+c+d = a+g_2 b+g_2 g_3 c+g_2 g_3 g_4 d = 0\}. \tag{5.2}$$

Because $\mathbb{C}[G]$ is semisimple [46], it splits into simple algebras $\mathbb{C}[G] = \bigoplus_{\rho \in \Delta} D_\rho$, where D_ρ is the simple subalgebras of $\mathbb{C}[G]$ corresponding to irreducible representation ρ. The splitting of the algebra gives a splitting of the cochain complex of $\mathbb{C}[G]$-modules $0 \to C^1 \to C^2$, hence a splitting of the cohomology:

$$H^1(M, \Sigma; \mathbb{C}) = \bigoplus_{\rho \in \Delta} H^1(\rho), \; H^1(\rho) = \{(a, b, c, d) \in D_\rho^4 : d^1(a, b, c, d) = 0\}. \tag{5.3}$$

Let L be the right ideal generated by $\{g_2 - 1, g_2 g_3 - 1, g_2 g_3 g_4 - 1\}$. The image of d^1 in $C^2(M, \Sigma; \mathbb{C})$ is

$$(1, 1)\mathbb{C}[G] \oplus (0, 1)L \subset (\mathbb{C}[G])^2 = C^2(M, \Sigma; \mathbb{C}).$$

This is because

$$\begin{aligned} d^1(a,b,c,d) &= (a+b+c+d, a+g_2b+g_2g_3c+g_2g_3g_4d) \\ &= (a+b+c+d, a+b+c+d) + (0,(g_2-1)b) + (0,(g_2g_3-1)c) + (0,(g_2g_3g_4-1)d) \\ &= (a+b+c+d)(1,1) + ((g_2-1)b + (g_2g_3-1)c + (g_2g_3g_4-1)d)(0,1) \end{aligned}$$

Now we show that $\mathbb{C}[G] = \mathbb{C} \oplus L$. Because $(1-a)+(1-b)a = 1-ba$, if g is a product of elements in $\{g_2, g_2g_3, g_2g_3g_4\}$ then $1-g \in L$. Also, because M is connected, $\{g_2, g_2g_3, g_2g_3g_4\}$ generates G, hence L is generated by all elements of the form $1-g$ for any $g \in G$, therefore $\mathbb{C}[G] = \mathbb{C} \oplus L$, where $\mathbb{C}$ is the trivial sub-algebra generated by $\sum_{g\in G} g$ [46]. Because $\mathbb{C}[G]$ is semisimple,

$$H^1(M,\Sigma;\mathbb{C}) = \ker(d^1) \to C^1(M,\Sigma;\mathbb{C}) \to im(d^1)$$

splits, hence we have

$$H^1(M,\Sigma;\mathbb{C}) = (\mathbb{C}[G])^4/(\mathbb{C}[G]\oplus L) = (\mathbb{C}[G])^2 \oplus \mathbb{C}. \tag{5.4}$$

Therefore, as G-module $H^1(\rho) \cong \mathbb{C}^3$ when ρ is the trivial representation, $H^1(\rho) \cong D_\rho^2$ if otherwise. Because G is abelian, $\dim_{\mathbb{C}} D_\rho = 1$, so $\dim_{\mathbb{C}} H^1(\rho) = 3$, if ρ is trivial, $\dim_{\mathbb{C}} H^1(\rho) = 2$, otherwise.

In the previous section we described elements in **Aff** as compositions of elementary affine diffeomorphisms $t_{\mathbf{h}}$, $s_{\mathbf{h}}$, $r_{g,\mathbf{h}}$, $f_{\mathbf{h}}$ and m_ψ, and elements in Γ as compositions of elementary affine diffeomorphisms $t_{\mathbf{h}}$, $s_{\mathbf{h}}$, $r_{g,\mathbf{h}}$ and $f_{\mathbf{h}}$. We will show the invariance of $H^1(\rho)$ under Γ by explicitly describing the action of elementary affine

diffeomorphisms. The maps from $H^1(M(G,\mathbf{h}),\Sigma;\mathbb{C})$ to some $H^1(M(G,\mathbf{h}'),\Sigma;\mathbb{C})$ induced by $t_{\mathbf{h}}$, $s_{\mathbf{h}}$, $r_{g,\mathbf{h}}$, $f_{\mathbf{h}}$ are as follows:

$$t^*_{\mathbf{h}}([a,b,c,d]) = [b,c,d,a] \tag{5.5}$$

$$s^*_{\mathbf{h}}([a,b,c,d]) = [-h_1 a, a+b, c, d+h_1 a] \tag{5.6}$$

$$r^*_{g,\mathbf{h}}([a,b,c,d]) = [ag,bg,cg,dg] \tag{5.7}$$

$$f^*_{\mathbf{h}}([a,b,c,d]) = [-a,-h_2h_3h_4d,-h_2h_3c,-h_2b]. \tag{5.8}$$

From equation (5.3) we know that they all preserve decomposition $H^1(*,\Sigma;\mathbb{C}) = \bigoplus_\rho H^1(\rho)$, hence all summands $H^1(\rho)$ are invariant under Γ.

Furthermore, m_ψ is a diffeomorphism from $M(G,\psi^{-1}\mathbf{h})$ to $M(G,\mathbf{h})$, and the map it induced from $H^1(M(G,\mathbf{h}),\Sigma;\mathbb{C})$ to $H^1(M(G,\psi(\mathbf{h})),\Sigma;\mathbb{C})$ is

$$\begin{aligned} &m^*_\psi([\sum_{g\in G} a_g g, \sum_{g\in G} b_g g, \sum_{g\in G} c_g g, \sum_{g\in G} d_g g]) \\ &\qquad = [\sum_{g\in G} a_g \psi^{-1}(g), \sum_{g\in G} b_g \psi^{-1}(g), \sum_{g\in G} c_g \psi^{-1}(g), \sum_{g\in G} d_g \psi^{-1}(g)] \end{aligned}$$

which, according to equation (5.3), would send $H^1(\rho)$ to $H^1(\psi^{-1}\rho)$. In other words, elements in **Aff** permute $H^1(\rho)$.

□

Remark 5.3.1. In certain situations $\Gamma =$ **Aff**. This happens when the g_j are all of different order, or when G is $\mathbb{Z}/n$, $n \geq 4$ and $\mathbf{g} = (1,1,1,n-3)$. In these cases $H^1(\rho)$ are all invariant under **Aff**. Our argument here is similar to, but not completely the same as those used in [37].

When G is non-abelian, we can define Γ' as the set of elements in $\mathbf{Aff}(M)$ that induce an inner automorphism on G, i.e. the set of elements in $\mathbf{Aff}(M)$ that can be written as compositions of t, s, r, f as well as m_ψ where ψ is an element of an inner automorphism of G. The argument above will show that $H^1(\rho)$ are invariant under Γ' and has dimension $2\dim(\rho)^2$ when ρ is non-trivial and dimension 3 when ρ is trivial.

5.4 The signature of the Hodge form

Now we define and calculate the signature of an invariant Hermitian form on $H^1(\rho)$ as in [50] and [12].

The Hodge form A_G on $H^1(M,\Sigma;\mathbb{C})$ is defined as the cup product [7] on (M,Σ) composed with coefficient pairing $\mathbb{C}\otimes\mathbb{C}\to\mathbb{C} : z\otimes z' \mapsto z\overline{z'}$, then normalized into a Hermitian form by multiplying $\frac{1}{2i}$.

$$H^1(M,\Sigma;\mathbb{C})\times H^1(M,\Sigma;\mathbb{C}) \xrightarrow{\smile} H^2(M,\Sigma;\mathbb{C}\otimes\mathbb{C}) \to H^2(M,\Sigma;\mathbb{C}) = \mathbb{C}.$$

More explicitly, let $(\cdot,\cdot)_G$ is the positive definite Hermitian norm on $\mathbb{C}[G]$ defined as

$$(\sum_g a_g g^{-1}, \sum_g b_g g^{-1})_G = \sum_g a_g \overline{b_g}$$

then

$$A_G([a,b,c,d],[a',b',c',d']) = \frac{1}{4i}((b,a')_G - (a,b')_G + (d,c')_G - (c,d')_G \\ -(h_2b,a')_G + (a,h_2b')_G - (h_2h_3h_4d,h_2h_3c')_G + (h_2h_3c,h_2h_3h_4d')_G). \tag{5.9}$$

Alternatively, if elements in $H^1(M,\Sigma;\mathbb{C})$ are represented by closed differential forms, A_G can be written as $A_G(\alpha,\beta) = \frac{1}{2i}\int_M \alpha\wedge\overline{\beta}$.

A_G is called the area form in [50], because when ω defines a flat structure on M, the signed area of this flat structure is $A_G(\omega,\omega)$. Unlike the Hodge norm defined by Eskin-Mirzakhani-Mohammadi, A_G vanishes on the *rel* subspace.

By definition A_G is invariant under the Γ-action. Furthermore, from (5.9) and the fact that different D_ρ are orthogonal under $(\cdot,\cdot)_G$, we know that $H^1(\rho)$ for different representation ρ are orthogonal to each other under A_G. When ρ is the trivial representation, $A_G = 0$ on $H^1(\rho)$.

Now we assume ρ to be a non-trivial representation. Because we will deal with Hermitian forms that may be degenerate, we denote by (n_0,n_+,n_-) the signature of a Hermitian form. Here n_0, n_+, n_- are the number of 0, positive and negative eigenvalues respectively.

We will prove the following theorem:

Theorem 5.4.1. *When $\rho \neq 1$, the signature of the area form A_G on $H^1(\rho)$, is $(n_0, \frac{\theta_2}{2\pi} - 1, \frac{\theta_1}{2\pi} - 1) = (4 - \frac{\theta_1+\theta_2}{2\pi}, \frac{\theta_2}{2\pi} - 1, \frac{\theta_1}{2\pi} - 1)$, where $\theta_1 = \sum_{j=1}^{4} arg(\rho(g_j))$, $\theta_2 = \sum_{j=1}^{4} arg(\rho(g_j)^{-1})$. The number n_0 is also the number of indices j such that $\rho(g_j) = 1$.*

Proof. In the case when $\rho(g_1g_2) = \rho(g_2g_3) = 1$ then $a = c$, $b = d$, and A_G is $2|G|$ times the area of parallelogram with side a and b, i.e. proportional to the cross product of two vectors on the complex plane, which has signature $(0, 1, 1) = (4 - \frac{\theta_1+\theta_2}{2\pi}, \frac{\theta_2}{2\pi} - 1, \frac{\theta_1}{2\pi} - 1)$.

Now we consider the case when $\rho(g_1g_2) \neq 1$ or $\rho(g_2g_3) \neq 1$. Without losing generality we assume $\rho(g_1g_2) \neq 1$. From equations (5.1), (5.3) we know that any $(a, b, c, d) \in H^1(\rho)$ satisfies

$$a + b + c + d = 0 \tag{5.10}$$

$$a + \rho(g_2)b + \rho(g_2g_3)c + \rho(g_2g_3g_4)d = 0 \tag{5.11}$$

. Because $\rho(g_3g_4) = \rho(g_1g_2)^{-1} \neq 1$, we can solve (b, d) from these two equations as linear functions of (a, c), i.e. rewrite these equations can be written as $(b, d) = (a, c)A$ where A is a 2-by-2 matrix.

Consider subspaces $H^1_a = \{(a, b, 0, d) \in H^1(\rho)\}$, $H^1_{a'} = \{(0, b, c, d) \in H^1(\rho)\}$, then by the previous arguments $\dim(H^1_a) = \dim(H^1_{a'}) = 1$ and $H^1(\rho) = H^1_a \oplus H^1_{a'}$. We will show that they are orthogonal subspaces under A_G. For any $(a, b, 0, d) \in H^1_a(\rho), (0, b', c', d') \in H^1_{a'}(\rho)$, because $(*, *)_G$ is G-invariant and $d^1(a, b, 0, d) =$

$d^1(0, b', c', d') = 0$, we have

$$\begin{aligned} A_G([a,b,0,d],[0,b',c',d']) &= \frac{1}{2i}(-(a,b')_G + (d,c')_G + (a,h_2b')_G - (h_2h_3h_4d, h_2h_3c')_G) \\ &= \frac{1}{2i}((b,b')_G + (d,b')_G - (d,b')_G - (d,d')_G - (h_2b, h_2b')_G \\ &-(h_2h_3h_4d, h_2b')_G + (h_2h_3h_4d, h_2h_3h_4d')_G + (h_2h_3h_4d, h_2b')_G) \\ &= 0 \end{aligned}$$

In other words, A_G is diagonalized under $H^1(\rho) = H^1_a \oplus H^1_{a'}$.

Now we show that the signature of A_G on H^1_a is $(3 - \frac{\theta_{1a}+\theta_{2a}}{2\pi}, \frac{\theta_{2a}}{2\pi} - 1, \frac{\theta_{1a}}{2\pi} - 1)$, where $\theta_{1a} = arg(\rho(g_1)) + arg(\rho(g_2)) + arg(\rho(g_3g_4))$, $\theta_{2a} = arg(\rho(g_1)^{-1}) + arg(\rho(g_2)^{-1}) + arg(\rho(g_3g_4)^{-1})$. From (5.10) and (5.11) we know that

$$H^1_a = \{t(\rho(g_2) - \rho(g_1^{-1}), \rho(g_1^{-1}) - 1, 0, \rho(g_2) - 1) : t \in D_\rho\} \tag{5.12}$$

. If $\rho(g_2) = 0$, equation (5.12) becomes $H^1_a = \{(t, -t, 0, 0) : t \in D_\rho\}$. If $\rho(g_1) = 0$, (5.12) becomes $H^1_a = \{(t, 0, 0, -t) : t \in D_\rho\}$. In both cases the signature is $(1, 0, 0) = (3 - \frac{\theta_{1a}+\theta_{2a}}{2\pi}, \frac{\theta_{2a}}{2\pi} - 1, \frac{\theta_{1a}}{2\pi} - 1)$. If neither $\rho(g_1)$ nor $\rho(g_2)$ is 1, $\theta_{1a} + \theta_{2a} = 6\pi$, and θ_{1a} is either 2π or 4π. From (5.9) and (5.12) we know that A_G is positive on H^1_a definite when $\theta_{1a} = 2\pi$ and negative definite on H^1_a when $\theta_{1a} = 4\pi$, i.e. the signature of A_G on H^1_a is $(3 - \frac{\theta_{1a}+\theta_{2a}}{2\pi}, \frac{\theta_{2a}}{2\pi} - 1, \frac{\theta_{1a}}{2\pi} - 1)$.

We can calculate the signature of A_G on $H^1_{a'}$ similarly. Because A_G is diagonalized under $H^1(\rho) = H^1_a \oplus H^1_{a'}$, the n_0, n_+ and n_- of A_G on $H^1(\rho)$ can be obtained by adding the n_0, n_+ and n_- of A_G on H^1_a and $H^1_{a'}$. □

5.5 The subgroup Γ_1 and triangle groups

In this section we introduce a subgroup Γ_1 of Γ of finite index, which is easier to work with than Γ. In Section 5.6, we will give a criteria for non-discreteness of the action of Γ by analyzing the action of this subgroup of finite index.

There is a homomorphism $D : \mathbf{Aff} \to SL(2,\mathbb{Z})$ that sends an affine diffeomorphism to its derivative. Because elements of **Aff** preserves Σ, $\ker(D)$ is finite. Consider two elements in Γ which are liftings of the horizontal and vertical Dehn twists of the pillowcase

$$\gamma_1 = s_{(g_1,g_2,g_3,g_4)} s_{(g_2,g_1,g_3,g_4)}$$

$$\gamma_2 = t_{(g_1,g_2,g_3,g_4)} s_{(g_2,g_3,g_4,g_1)} s_{(g_3,g_2,g_4,g_1)} t^{-1}_{(g_1,g_2,g_3,g_4)}.$$

$D\gamma_1$ and $D\gamma_2$ generates the level 2 congruence subgroup of $SL(2,\mathbb{Z})$, hence the group generated by them is a subgroup of **Aff** of finite order. From (5.5), (5.6) we have:

$$\gamma_1^*(a,b,c,d) = (g_1g_2a, b + a - g_1a, c, d + g_1a - g_1g_2a) \tag{5.13}$$

$$\gamma_2^*(a,b,c,d) = (a + g_2b - g_2g_3b, g_2g_3b, c + b - g_2b, d) \tag{5.14}$$

Denote the group generated by γ_1 and γ_2 as Γ_1. When restricted to $H^1(\rho)$,

$$\gamma_1^*(a,b,c,d) = (\rho(g_1g_2)a, b + a - \rho(g_1)a, c, d + \rho(g_1)a - \rho(g_1g_2)a) \tag{5.15}$$

$$\gamma_2^*(a,b,c,d) = (a + \rho(g_2)b - \rho(g_2g_3)b, \rho(g_2g_3)b, c + b - \rho(g_2)b, d) \tag{5.16}$$

. When $\rho = 1$ is the trivial representation, the Γ_1 action on $H^1(\rho)$ is trivial. When ρ is non-trivial, the Γ action on $H^1(\rho) = \mathbb{C}^2$ induces an action on $\mathbb{CP}^1$ under projectivization. The map on $\mathbb{CP}^1$ induced by γ_1 is parabolic if and only if $\rho(g_1 g_2) = 1$. Similarly, γ_2 is parabolic if and only if $\rho(g_2 g_3) = 1$. If they are not parabolic they are elliptic.

Remark 5.5.1. Furthermore, when $\rho(g_2) = 1$ and all other $\rho(g_j) \neq 1$, the Γ_1 action $H^1(\rho)$ is not semisimple. We can see this as follows: by equations (5.15) and (5.16), $(1, -1, 0, 0)$ is the only common eigenvector of γ_1^* and γ_2^* in $H^1(\rho)$, hence $H^1_a(\rho) = \{(t, -t, 0, 0)\}$ is the only 1-dimensional subspace of $H^1(\rho)$ invariant under Γ_1, i.e. in this case the Γ_1 action on $H^1(\rho)$ is not semisimple. $H^1_a(\rho)$ is also the kernel of the projection $H^1(M, \Sigma; \mathbb{C}) \to H^1(M; \mathbb{C})$ restricted to $H^1(\rho)$.

Hence, we have:

Proof of Theorem 5.1.2. (1),(3) follows from Theorem 5.4.1. (2) follows from Remark 5.5.1. □

The Hodge norm A_G on $H^1(\rho)$ induces a metric, hence a geometric structure on the projectivization $\mathbb{P}(H^1(\rho)) = \mathbb{CP}^1$ invariant under the Γ-action. When A_G is positive definite or negative definite, it induces a spherical structure on $\mathbb{CP}^1$. When A_G has signature $(1, 0, 1)$, it induces a Euclidean structure on $\mathbb{CP}^1 - [0 : 1]$. When A_G has signature $(1, 1, 0)$, it induces a Euclidean structure on $\mathbb{CP}^1 - [1 : 0]$. Finally, when the signature of A_G is $(0, 1, 1)$, it induces a hyperbolic structure on a

disc D in $\mathbb{P}H^1(\rho)$, which consists of the image $\{\alpha \in H^1(\rho) : A(\alpha, \alpha) > 0\}$. The case (3) of Theorem 5.1.2 corresponds to the elliptic and parabolic cases, while case (2) of Theorem 5.1.2 corresponds to the Euclidean case. In all these cases, we will show that the action of Γ_1 is through an index-2 subgroup of the triangle group, which proves Theorem 5.1.3.

Proof of Theorem 5.1.3. In the spherical case, all the elements in Γ_1 are rotations hence has a pair of fixed points. Let P_1 be a fixed point of γ_1, P_2 be a fixed point of γ_2, P_3 be a fixed point of $\gamma_2^{-1}\gamma_1$, let $\Delta P_1P_2P_3$ and $\Delta P_1P_2\gamma_1(P_3)$ be spherical triangles formed by the shortest geodesics between these points, then they are related by reflection along P_1P_2, and γ_1 can be presented as reflection along first P_1P_3 then P_1P_2, while γ_2 is reflection along P_2P_3 followed by reflection along P_1P_2, hence Γ_1 acts through a subgroup of the triangle reflection group T corresponding to $\Delta P_1P_2P_3$. Because Γ_1 action preserves orientation, its image under the action is contained in the index-2 subgroup consisting of compositions of even number of reflections along the three sides of the triangle.

On the other hand, a reflection along P_1P_2 then P_1P_3 is the same as the action of γ_1^{-1}, a reflection along P_1P_2 then P_2P_3 is the same as the action γ_2^{-1}, a reflection along P_1P_3 then P_2P_3 is the same as the action $\gamma_2^{-1}\gamma_1$, and a reflection along P_2P_3 then P_1P_3 is the same as the action $\gamma_1^{-1}\gamma_2$, the composition of any sequence of even number of reflections along P_1P_2, P_2P_3 and P_1P_3 can be written as the action of a composition of γ_1, γ_2 and their inverses, hence Γ_1 acts through the index-2 sub-

group of T consisting of compositions of even number of reflections.

In the euclidean case the argument is the same. In the hyperbolic case, when γ_1, γ_2 and $\gamma_2^{-1}\gamma_1$ are all elliptic elements, we choose fixed points P_1, P_2 and P_3 all in the disc D described above, then the same argument would work.

Finally, in the hyperbolic case, in which γ_1, γ_2 or $\gamma_2^{-1}\gamma_1$ is parabolic, choose the corresponding P_i to be the unique fixed point on ∂D, then the sides ending at P_i become geodesic rays in D that approaches P_i on the ideal boundary. The same argument will show that the Γ_1-action is through an index-2 subgroup of a triangle reflection group with certain angles being 0.

□

Suppose elliptic element $\gamma \in PGL(2,\mathbb{C})$ has a fixed point $P \in \mathbb{CP}^1$, then by conjugating with an element in $PGL(2,\mathbb{C})$ we can make $P = [1,0]$ and $\gamma = \begin{pmatrix} e^{\sqrt{-1}\theta_1} & 0 \\ 0 & e^{\sqrt{-1}\theta_2} \end{pmatrix}$, which in the tangent space $T_P\mathbb{CP}^1$ induces a rotation of angle $\theta_2 - \theta_1$. Hence, an elliptic element in Γ_1 induces a rotation and the rotation angle is the argument of the quotient of the 2 eigenvalues, hence can be calculated with (5.15) and (5.16). The angles of the triangle at P_1, P_2 and P_3 are half of the rotation angles of γ_1, γ_2^{-1} and $\gamma_2^{-1}\gamma_1$ respectively. We will describe these triangle groups and their applications in the next two sections.

5.6 The spherical case and polyhedral groups

In this section we will describe the spherical case, and in the next section we will describe the remaining cases.

When A_G is positive definite or negative definite, the generators of Γ_1, γ_1 and γ_2, act as finite order rotations with different fixed points, and their orders are the orders of $\rho(g_1g_2)$ and $\rho(g_2g_3)$ in $\mathbb{C}^*$ respectively, hence by the ADE classification [13] of finite subgroups of $SO(3)$ we know that if both the orders of $\rho(g_1g_2)$ and $\rho(g_2g_3)$ are greater than 5 the action of Γ on $H^1(\rho)$ can not factor through a discrete group.

Proof of Proposition 5.1.4 and Remark 5.1.1. : Let G be the subgroup of $(\mathbb{Z}/120)^3$ spanned by $g_1 = (20, 0, 0)$, $g_2 = (0, 15, 0)$, $g_3 = (0, 0, 12)$, $g_4 = (100, 105, 108)$, $\mathbf{g} = (g_1, g_2, g_3, g_4)$, $M = M(G, \mathbf{g})$, $\rho(g_1) = e^{\pi i/3}$, $\rho(g_2) = e^{\pi i/4}$, $\rho(g_3) = e^{\pi i/5}$, $\rho(g_4) = e^{73i\pi/60}$. Then by Theorem 5.1.1 and Remark 5.3.1 $H^1(\rho)$ is invariant under **Aff** with an invariant complement, by Section 5.4 the Hodge form is positive definite on $H^1(\rho)$, and by the argument above the **Aff** action on $H^1(\rho)$ is not discrete. In other words, M and the decomposition $H^1(M, \Sigma; \mathbb{C}) = H^1(\rho) \oplus H^1(\overline{\rho}) \oplus (\bigoplus_{\rho' \neq \rho, \overline{\rho}} H^1(\rho'))$ satisfy all the conditions mentioned in Proposition 5.1.4. Furthermore, the tangent space of the $GL(2, \mathbb{R})$ orbit is $H^1(\rho_t)$ where $\rho_t(g_j) = -1$ for $j = 1, 2, 3, 4$. Because $\rho_t \neq \rho$, $\rho_t \neq \overline{\rho}$, the decomposition also satisfy conditions in Remark 5.1.1. □

Furthermore, by Theorem 5.1.3 and [9], we can list all possible 4-tuples $(\rho(g_1), \rho(g_2), \rho(g_3), \rho(g_4))$ such that the Γ_1 action on $\mathbb{P}(H^1(\rho)) = \mathbb{CP}^1$ factors through a finite group. Denote the arguments of $\rho(g_j)$ as $2t_j\pi$, $j = 1, \ldots 4$, then the Γ_1 action is finite if and only if t_1, t_2, t_3, t_4 is a permutation of one of the 4-tuples in the table below:

Table 5.1: Representation ρ that make **Aff** action on $H^1(\rho)$ finite

t_1	t_2	t_3	t_4	Group
d/2n	d/2n	(n-d)/2n	(n-d)/2n	Dihedral group
1/12	1/4	1/4	5/12	Tetrahedral group
1/24	5/24	7/24	11/24	Octahedral group
1/60	11/60	19/60	29/60	Icosahedral group
1/6	1/6	1/6	1/2	Tetrahedral group
1/12	1/6	1/6	7/12	Octahedral group
1/30	19/30	1/6	1/6	Icosahedral group
1/30	3/10	3/10	11/30	Icosahedral group
1/20	3/20	7/20	9/20	Icosahedral group
1/15	2/15	4/15	8/15	Icosahedral group
1/10	3/10	3/10	3/10	Icosahedral group
1/10	1/10	7/30	17/30	Icosahedral group
1/10	1/10	1/10	7/10	Icosahedral group
7/60	13/60	17/60	23/60	Icosahedral group
1/6	1/6	7/30	13/30	Icosahedral group
(2n-d)/2n	(2n-d)/2n	(n+d)/2n	(n+d)/2n	Dihedral group
7/12	3/4	3/4	11/12	Tetrahedral group
13/24	19/24	17/24	23/24	Octahedral group
31/60	41/60	49/60	59/60	Icosahedral group
1/2	5/6	5/6	5/6	Tetrahedral group
5/12	5/6	5/6	11/12	Octahedral group
5/6	5/6	11/30	29/30	Icosahedral group
19/30	7/10	7/10	29/30	Icosahedral group
11/20	13/20	17/20	19/20	Icosahedral group
7/15	11/15	13/15	14/15	Icosahedral group
7/10	7/10	7/10	9/10	Icosahedral group
13/30	23/30	9/10	9/10	Icosahedral group
3/10	9/10	9/10	9/10	Icosahedral group
37/60	43/60	47/60	53/60	Icosahedral group
17/30	23/30	5/6	5/6	Icosahedral group

Here d and n are positive integers, and the last column shows the discrete subgroup of $SO(3)$ it corresponds to.

Examples of M and ρ that satisfies the conditions needed for Proposition 5.1.4 and Remark 5.1.1 can therefore be built from any 4-tuple of positive rational numbers not on the above list that sum up to 1 or 3. For example, $(1/8, 1/8, 1/8, 5/8)$ is not on the list, so let $G = \mathbb{Z}/8$, $g_1 = g_2 = g_3 = 1$, $g_4 = 5$, $\rho(g_1) = \rho(g_2) = \rho(g_3) = e^{\pi i/4}$, $\rho(g_4) = e^{5\pi i/4}$ satisfies those conditions. This is an abelian cover of flat pillowcase that satisfy those conditions with the smallest number of squares. It has 16 squares in total and is in the stratum $H(3, 3, 3, 3)$.

Explicit elements of $N = H^1(\rho)$ and $Re(N) = Re(H^1(\rho))$ can also be calculated by solving (5.10) and (5.11). For example, in the abovementioned $G = \mathbb{Z}/8$, $g_1 = g_2 = g_3 = 1$, $g_4 = 5$, $\rho(g_1) = \rho(g_2) = \rho(g_3) = e^{\pi i/4}$, $\rho(g_4) = e^{5\pi i/4}$ case, $\alpha \in H^1(M, \Sigma, \mathbb{R})$, $\alpha(e_k^1) = -2\cos(\pi/8)\cos(k\pi/4)$, $\alpha(e_k^2) = \cos(\pi/8 + k\pi/4)$, $\alpha(e_k^3) = 0$, $\alpha(e_k^4) = \cos(\pi/8 - k\pi/4)$ is an element in $Re(H^1(\rho))$.

5.7 The hyperbolic and Euclidean cases and triangle groups

In this section we complete the description of Γ_1-action by describing the signature $(0, 1, 1)$, $(1, 0, 1)$, $(1, 1, 0)$ cases as triangle groups. In the $(0, 1, 1)$ case, $\sum_j arg(\rho(g_j)) = 4\pi$. Without losing generality we assume $arg(\rho(g_1))+arg(\rho(g_2)) \geq 2\pi$,

$arg(\rho(g_2)) + arg(\rho(g_3)) \geq 2\pi$.

By calculation based on the observations in Section 5.5, γ_1 acts on D as a rotation by $arg(\rho(g_1g_2))$ when $\rho(g_1g_2) \neq 1$ and as a parabolic transformation when $\rho(g_1g_2) = 1$, γ_2 acts on D as a rotation by $arg(\rho(g_2g_3))$ when $\rho(g_2g_3) \neq 1$ and as a parabolic transform when $\rho(g_2g_3) = 1$. Furthermore, γ_1 and γ_2 generate an index 2 subgroup of a triangle group, and the angles of the triangle are $|\pi - (arg(\rho(g_1)) + arg(\rho(g_2)))/2|$, $|\pi - (arg(\rho(g_2)) + arg(\rho(g_3)))/2|$ and $|\pi - (arg(\rho(g_1)) + arg(\rho(g_3)))/2|$. [55] has done the same calculation and based on it has calculated the Lyapunov exponents from the area of this triangle.

When the signature of A_G is $(1, 1, 0)$ or $(1, 0, 1)$, only one $\rho(g_j)$ is equal to 1. Without losing generality assume $\rho(g_2) = 1$, then $(a, b, c, d) \mapsto b/a$ sends $H^1(\rho)$ to $\overline{\mathbb{C}}$, and under this map Γ_1 acts on $\mathbb{C} = \overline{\mathbb{C}} - \{\infty\}$ as an index-2 subgroup of a Euclidean triangle group. The angles of the triangle are $arg(\rho(g_1))/2$, $arg(\rho(g_3))/2$ and $arg(\rho(g_4))/2$ when

$$arg(\rho(g_1)) + arg(\rho(g_3)) + arg(\rho(g_4)) = 2\pi$$

i.e. when the signature of A_G is $(1, 1, 0)$. The angles of the triangles are $\pi - arg(\rho(g_1))/2$, $\pi - arg(\rho(g_3))/2$ and $\pi - arg(\rho(g_4))/2$ when

$$arg(\rho(g_1)) + arg(\rho(g_3)) + arg(\rho(g_4)) = 4\pi$$

i.e. when the signature of A_G is $(1, 0, 1)$.

When two of the four $\rho(g_j)$ are equal to 1, then the Γ_1 action on $H^1(\rho)$ factors through a finite abelian group. Finally, when $\rho = 1$, the Γ_1 action on $H^1(\rho)$ is trivial, and the Γ-action is through a finite permutation group.

CHAPTER 6

APPLICATION ON BOUW-MÖLLER SURFACES

6.1 Introduction

Square-tiled translation surfaces are lattice surfaces because they are branched covers of the flat torus with a single branched point. Many non-square-tiled examples of lattice surfaces arise from "deforming" certain square-tiled surfaces. These include Veech's regular n-gon [52], Ward's surfaces [54], and, more generally, the Bouw-Möller surfaces, which were discovered by Bouw-Möller [6]. All of them arise from deforming abelian normal covers of the flat pillowcase. Hooper [27] gave a translation-surface-theoretic description of these examples by introducing a class of Thurston-Veech diagrams which he called "grid graphs", and Wright [56] proved the equivalence of the construction in [27] and [6]. Here we formalize a "geometric" Bouw-Möller construction by studying a class of lattice surfaces that arise from deforming certain marked square-tiled surfaces, and the possible geometric obstacles for such deformation. Our approach leads to a new class of Thurston-Veech diagrams similar to Hooper's but it does not result in new lattice surfaces. We hope that it will provide some insights on the reasons that makes Bouw-Möller's construction possible.

We will show that:

Theorem 6.1.1. *If a lattice surface arises from deforming an abelian branched cover of flat pillowcase M using a relative cohomology class α, its affine diffeomorphism group is commensurable with the affine diffeomorphism group of M, and the deformation also preserves the Thurston-Veech structure in the two diagonal directions, then this surface must have one of the 3 types of Thurston-Veech structures which will be described in Section 6.4 and 6.5. As a consequence, the surface must be one of the followings cases:*

1. *a branched cover of the regular $2n$-gon branched at the cone point.*
2. *a branched cover of a Bouw-Möller surface.*
3. *a branched cover of the regular n-gon branched at the mid-point of edges.*

Given a translation surface (M, Σ) with a polygonal decomposition, and a 1-form $\alpha \in H^1(M, \Sigma; \mathbb{C})$, we now define the "deformation" of (M, Σ) using α. We have:

Lemma 6.1.2. *Let (M, Σ) be a square-tiled translation surface. If a cohomology class $\alpha \in H^1(M, \Sigma; \mathbb{C})$ evaluated on the four sides of any square in M are the coordinates of the four sides of a convex quadrilateral with a non-negative area, then there is a translation surface X with certain points identified, and a degree 1 map from M to X, such that the pull back of the translation structure of X is defined by α.*

Proof. We construct X and the map $M \to X$ as follows: every 2-cell B in M is mapped to a convex, possibly degenerate, quadrilateral on $\mathbb{C}$ with non-negative

area, the coordinate of its four sides are given by α evaluated on the four sides of B. Each of the four sides of B is sent to the respective side of the quadrilateral linearly. The sides of those quadrilaterals are then glued to each other by isometry to form the space X. □

Definition 6.1.1. We call X and the degree 1 map $i : M \to X$ in the previous lemma a *deformation* of M using α.

For example, if we let $M = M(\mathbb{Z}/30, (1, 11, 29, 19))$, α be a 1-form corresponding to $(5, 3)$ Bouw-Möller surface (which we will describe in Section 6.5), then the deformation consists of four translation surfaces glued together at their cone points as in Figure 6.1.

Labels $a \dots h$ show the gluing of edges, and numbers show the image of 2-cells in M. Some of these images are convex quadrilaterals, some are triangles, and some (1,5,11,15 in Figure 6.1) are collapsed into line segments.

The metric completion of $X - i(\Sigma)$ may have multiple connected components. Also, the deformation depends not only on α but also on the choice of cell structure on (M, Σ). We denote by $M \to X(\alpha)$ the deformation of M using α.

Definition 6.1.2. Let $i\colon (M, \Sigma) \to (X, \Sigma')$ be a deformation of (M, Σ). We say a homeomorphism $g\colon (M, \Sigma) \to (M, \Sigma)$ acts on X through an affine diffeomorphism

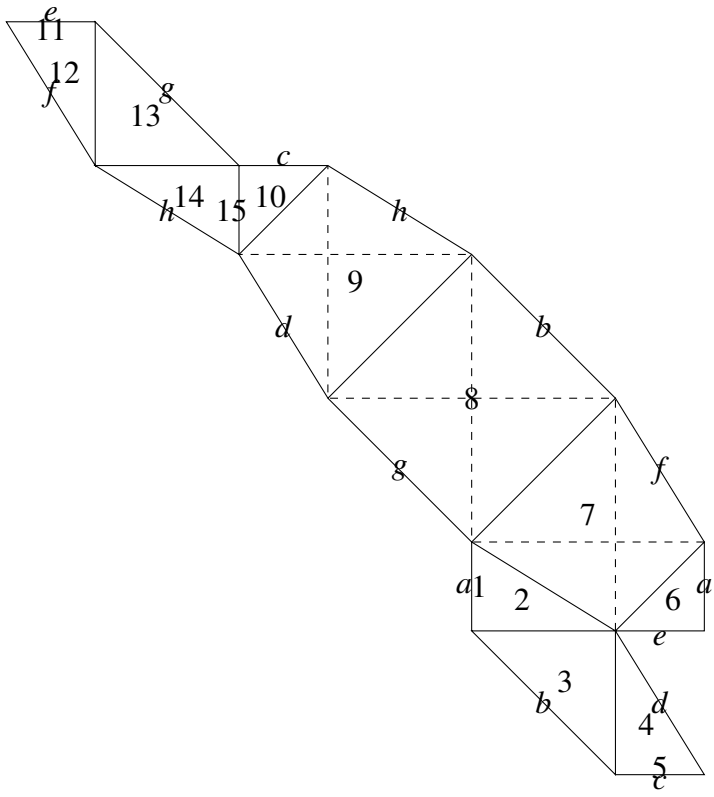

Figure 6.1: The $(5, 3)$ Bouw-Möller surface.

$f : X \to X$, if the translation structure of X pulled back by $i \circ g$ and $f \circ i$ determine the same cohomology class in $H^1(M, \Sigma; \mathbb{C})$.

Remark 6.1.1. In the situation we will consider, we assume that a finite-index subgroup Γ' of the affine diffeomorphism group $\mathbf{Aut}(M)$ acts on lattice surface X through a finite index subgroup of $\mathbf{Aut}(X)$. Hence by Definition 6.1.2, Γ' preserves $N(\alpha) = span_{\mathbb{C}}(\alpha, \overline{\alpha})$, and the action is through a lattice in $U(1, 1)$.

The decomposition $H^1(M, \Sigma) = \bigoplus_\rho H^1(\rho)$ is Γ-invariant. By replacing Γ' with $\Gamma' \cap \Gamma$, we will, from now on, always assume that Γ' is a subgroup with finite index

of Γ without loss of generality. As a consequence, the projection from $H^1(M, \Sigma)$ to each $H^1(\rho)$ is Γ'-equivariant. If we also take Schur's Lemma into account, we get:

Proposition 6.1.3. *Under the assumption of Remark 6.1.1, the projection from $N(\alpha) = span_{\mathbb{C}}(\alpha, \overline{\alpha})$ to $H^1(\rho)$ is either 0, or a Γ'-isomorphism. In the latter case Γ' acts on $H^1(\rho)$ through a lattice in $U(1,1)$.*

□

From this we know:

Corollary 6.1.1. *Under the assumption of Remark 6.1.1,*

$$N(\alpha) \subseteq \bigoplus_{H^1(\rho) \text{ is isomorphic to } N(\alpha) \text{ as } \Gamma'\text{-module}} H^1(\rho)$$

□

In section 6.2 we review the concept of a Thurston-Veech structure. In section 6.3 we review the discrete Fourier transform which is needed for the proof of Theorem 1.1, and in section 6.4 and 6.5 we prove Theorem 6.1.1.

6.2 Thurston-Veech diagrams

Recall that a Thurston-Veech structure [51] on a translation surface consists of two tuples of positive integers $\{r_i\}$ and $\{r'_j\}$, and a pair of transverse cylinder decompositions $\{C_i\}$ and $\{C'_j\}$, with moduli $\{M_i\}$ and $\{M'_j\}$ respectively, such that

$M_{i_1}/M_{i_2} = r_{i_1}/r_{i_2}$ and $M'_{j_1}/M'_{j_2} = r'_{j_1}/r'_{j_2}$. A Thurston-Veech structure on a translation surface induces two parabolic affine diffeomorphisms γ and γ' given by two multitwists on $\{C_i\}$ and $\{C'_j\}$ respectively. The intersection configuration of the two cylinder decompositions can be represented by a Thurston-Veech diagram, which is a ribbon graph constructed as follows: each vertex represents a cylinder, an edge between two vertices stands for an intersection of two cylinders, and the cyclic order among all edges associating with each vertex encodes the order of these intersections on the cylinder represented by this vertex.

On a square-tiled surface M, the two diagonal directions are periodic, and cylinder decompositions on these two directions form a Thurston-Veech structure. We call the cylinders from the bottom-left to top-right $\{C_i\}$, and the cylinders from the bottom-right to top-left $\{C'_j\}$. The Thurston-Veech diagram that arises from this Thurston-Veech structure can be constructed explicitly as follows: we get a square-tiled coned flat surface by gluing the squares with the same edge pairing as in M but with all the gluing directions flipped, which we denote by $\mathcal{F}M$. Now each vertex in the square tiling of $\mathcal{F}M$ corresponds to a cylinder in M formed by triangles, as illustrated in Figure 6.2.

Here the 4 triangles I, II, III and IV that form a cylinder in the bottom-left to top-right direction become the 4 triangles around P after the re-gluing, just as triangles that form the cylinder between the two red arrows become the 4 triangles

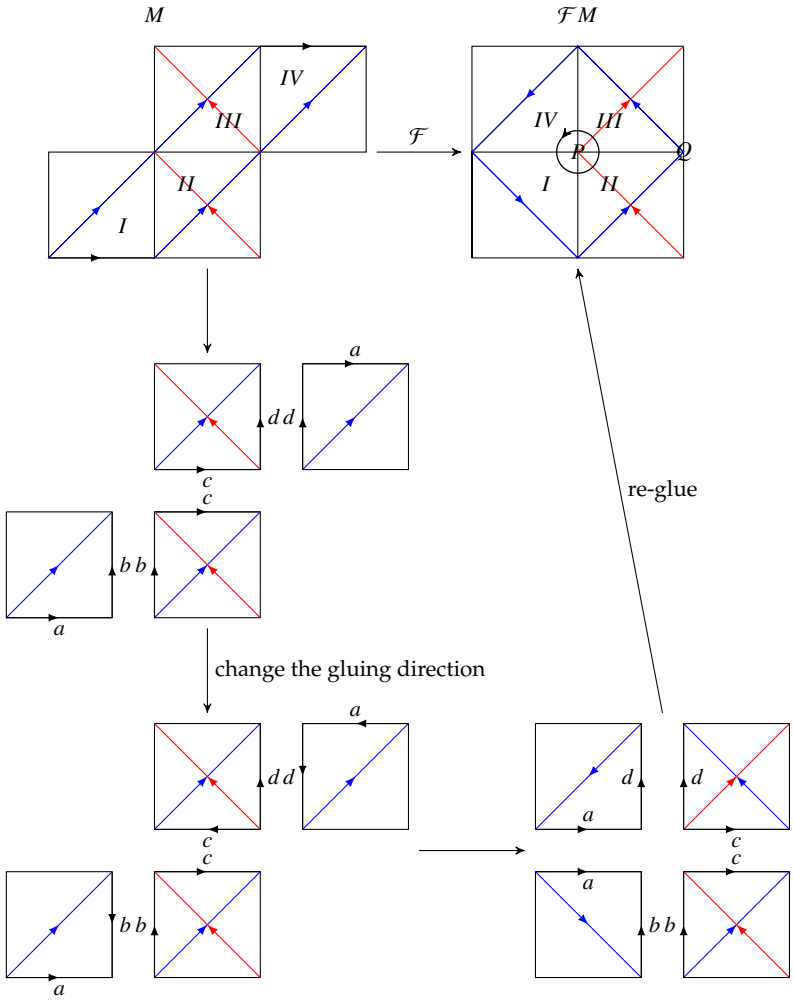

Figure 6.2: Constructing Thurston-Veech diagram by flipping.

around Q after the re-gluing. Furthermore, the intersection of these two cylinders is represented by the edge PQ. The cyclic orders among the edges can be seen from the blue and red arrows. Hence, the Thurston-Veech diagram is the 1-skeleton of $\mathcal{F}M$, with the cyclic orders in clockwise and counterclockwise direction alternatively by columns as illustrated in Figure 6.3.

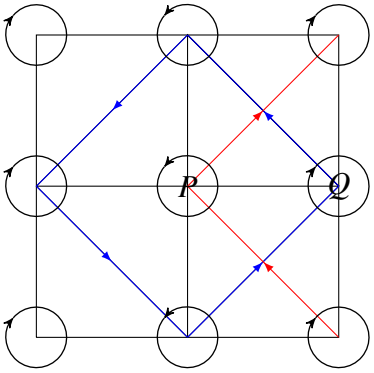

Figure 6.3: The resulting Thurston-Veech diagram.

In our case when M is a cover of the pillowcase, $\mathcal{F}M$ is always orientable. Because in the gluing process described above, any two adjacent squares are always glued with orientation reversed, we can define an orientation on $\mathcal{F}M$ as either the orientation of all the B_g^1 after the regluing, or the opposite of the orientation of all B_g^2 after regluing. Also, because M is a normal cover, all cylinders in the same diagonal direction have the same circumference and width. Hence, they must have the same moduli, i.e. $r_i = r'_j = 1$ for all i, j.

Definition 6.2.1. We say that a 1-form $\alpha \in H^1(M, \Sigma)$ *preserves* a cylinder decomposition $\{C_i\}$ on M, if α evaluated on all paths contained in all the boundary curves of these cylinders are parallel. We say α *preserves* a Thurston-Veech structure, if it preserves both cylinder decompositions, and the multitwists γ, γ', which are induced by to the Thurston-Veech structure, preserve $span_{\mathbb{C}}(\alpha, \overline{\alpha})$.

A cohomology class α that satisfies the assumption of Remark 6.1.1 must preserve at least two parabolic elements, and, thereby, two cylinder decompositions.

Here, we assume that it preserves the two cylinder in the two diagonal directions of M. We denote by $\mathcal{L}(M,\Sigma)$ the set of elements of $H^1(M,\Sigma;\mathbb{C})$ that preserves the two cylinder decomposition in the diagonal directions, and by $\mathcal{N}(M,\Sigma)$ the set of those elements in $\mathcal{L}$ that further preserve the Thurston-Veech structure in the diagonal directions. Furthermore, we denote by $\mathcal{L}'$ and $\mathcal{N}'$ the set of those elements in $\mathcal{L}$ and $\mathcal{N}$ whose value on bottom-left-to-top-right diagonals are in $\mathbb{R}$, and whose value on bottom-right-to-top-left diagonals are in $\sqrt{-1}\mathbb{R}$. Any element in $\mathcal{L}$ or $\mathcal{N}$ can be made into an element in $\mathcal{L}'$ or $\mathcal{N}'$ after an affine transformation.

The circumference, width and moduli of C_i under α is defined as the base, height and moduli of the parallelogram formed by α evaluated on the boundary circle and α evaluated on a path that crosses the cylinder once from right to left.

Let $V = V(\mathcal{F}M)$ be the space of real valued functions on the vertices of $\mathcal{F}M$. Let $\Psi : \mathcal{L}' \to V$ be the map defined as follows: given any element $\alpha \in \mathcal{L}'$, $\Psi(\alpha)$ sends a vertex to the width under α of the cylinder it represents. It is a bijective map. Because $r_i = r'_j = 1$, the fact that multitwists γ and γ' preserve $span_{\mathbb{C}}(\alpha, \overline{\alpha})$ implies that any C_i with non-zero width have the same moduli, and those with width 0 also have 0 circumference. By [51], we can make all the cylinders to have either identical moduli $\lambda > 0$ or zero width and zero circumference after an affine action, and get:

Lemma 6.2.1. *[51] Let A be the adjacency matrix of the Thurston-Veech diagram, then*

up to an affine action, α satisfies $A(\Psi(\alpha)) = \lambda\Psi(\alpha)$.

□

When $\alpha \in \mathcal{L}'$, the assumption of Lemma 6.1.2 can be further rewritten as a condition on the image of Ψ:

Lemma 6.2.2. *Assuming $\alpha \in \mathcal{L}'$, the assumption of Lemma 6.1.2 is equivalent to the fact that no pair of adjacent vertices of $\mathcal{F}M$ can be assigned values of opposite signs by $\Psi(\alpha)$, and there is an edge such that neither of its end points are assigned* 0.

Proof. If assumption of Lemma 6.1.2 holds, any square B_j^k will be sent to a convex quadrilateral with non-negative area under the flat structure defined by α. The two diagonals of this quadrilateral cut it into 4 small triangles of non-negative area. If two non-degenerate cylinders in the cylinder decompositions described above intersect, its intersection must be a rectangle formed by two of those small triangles hence must have non-negative signed area, i.e. $\Psi(\alpha)$ can not assign values of opposite signs for any pair of adjacent vertices. At least one of these rectangles must have positive area, hence there is at least one pair of adjacent vertices such that $\Psi(\alpha)$ is non-zero on both.

On the other hand, if $\Psi(\alpha)$ does not assign values of opposite signs for any pair of adjacent vertices, we can build a translation surface X as follows: each parallelogram formed by the intersection of some C_i and C'_j are sent to a $\Psi(\alpha)(v_i)$-by-$\Psi(\alpha)(v_j)$ rectangle, where v_i and v_j are vertices in $\mathcal{F}M$ that represent C_i and C'_j

respectively. As illustrated in Figure 6.4, the sides of these rectangles are glued in the same order as the gluing of the parallelograms on M, which means that α satisfies the assumption of Lemma 6.1.2.

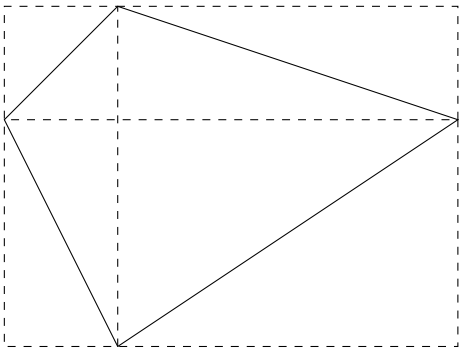

Figure 6.4: Condition for the convexity of the quadrilateral.

□

Remark 6.2.1. When α satisfies the assumption of Lemma 6.1.2, we can decompose $X(\alpha)$ into a union of (possibly degenerated) cylinders in two ways, and choose the map $i : M \to X(\alpha)$ such that these two cylinder decompositions are the images of $\{C_i\}$ and $\{C'_j\}$.

Let $\mathcal{S}$ be the category of square-tiled surfaces with morphisms being continuos maps that send squares isometrically to squares. Our construction of $\mathcal{F}M$, $\mathcal{L}(M)$, $\mathcal{N}(M)$ and $V(\mathcal{F}M)$ from M are functorial. More precisely,

Lemma 6.2.3. *A $\mathcal{S}$-morphism $\xi : M \to M'$ induces canonically a $\mathcal{S}$-morphism $\mathcal{F}\xi : \mathcal{F}M \to \mathcal{F}M'$, $\xi^* : \mathcal{L}'(M') \to \mathcal{L}'(M)$, and $(\mathcal{F}\xi)^* : V(\mathcal{F}M') \to V(\mathcal{F}M)$ and the following*

diagram commute:

$$\begin{array}{ccc} \mathcal{L}'(M') & \to & \mathcal{L}'(M) \\ \downarrow \Psi & & \downarrow \Psi \\ V(\mathcal{F}M') & \to & V(\mathcal{F}M) \end{array}$$

Furthermore, ξ^* sends $\mathcal{N}'$ to $\mathcal{N}'$.

□

Remark 6.2.2. $(\mathcal{F}\xi)^*$ can be described more concretely as follows: for any $f \in V(\mathcal{F}M')$, any vertex in $\mathcal{F}M$, $(\mathcal{F}\xi)^* f(v) = f(\mathcal{F}\xi(v))$ if $\mathcal{F}\xi$ preserves the cyclic order among the edges associated to v, and $(\mathcal{F}\xi)^* f(v) = -f(\mathcal{F}\xi(v))$ if it reverses the cyclic order.

Remark 6.2.3. $\mathcal{F}^2$ is the same as the identity functor $1_{\mathcal{S}}$. Hence $\mathcal{F} : \mathcal{S} \to \mathcal{S}$ is an isomorphism.

Now we consider the question of finding $\alpha \in \mathcal{N}'$ that satisfies the assumption of Lemma 6.1.2 and that a subgroup of $\mathbf{Aff}(M)$ of finite index acts on $N(\alpha)$ as a lattice. We say such α satisfies property (L). Now we analyze all possible 1-forms with property (L).

Let e be the identity element in G. Let γ_1 be the element in Γ that preserve the button-right corner of B^1_e and has derivative $\begin{pmatrix} 1 & -2 \\ 0 & 1 \end{pmatrix}$; let γ_2 be the element in

Γ that preserve the button-right corner of B_e^1 and has derivative $\begin{pmatrix} 1 & 0 \\ -2 & 1 \end{pmatrix}$; let γ_3 be the element in Γ that preserve the button-right corner of B_e^1 and has derivative $\begin{pmatrix} 3 & -2 \\ 2 & -1 \end{pmatrix}$, and let γ_4 be the element in Γ that preserve the button-right corner of B_e^1 and has derivative $\begin{pmatrix} 3 & 2 \\ -2 & -1 \end{pmatrix}$. These elements are liftings of the Dehn twists in the horizontal, vertical and the two diagonal directions on P.

Let $\alpha \in \mathcal{N}'$. By Definition 6.2.1, some power of γ_3 and γ_4 acts on $X(\alpha)$ as parabolic affine automorphisms, hence their action on $N(\alpha)$ are parabolic. Because a power of γ_3 acts on $H^1(\rho)$ as parabolic map if and only if $\rho(g_1g_3) = 1$, by Corollary 6.1.1, $N(\alpha) \subset \oplus_{\rho\in\{\rho:\rho(g_1)\rho(g_3)=1\}} H^1(\rho)$. Hence, α is the pull back of some $\alpha' \in \mathcal{N}'(M(G/(g_1g_3), \mathbf{g}))$ by a $ord_G(g_1g_3)$-fold branched cover $M \to M_1 = M(G/(g_1g_3), \mathbf{g})$. Hence $X(\alpha)$ is a branched cover of $X(\alpha')$ branching at $i(\Sigma) \subset \Sigma'$.

Because the deck group of M_1 is $G_1 = G/(g_1g_3)$, $g_1g_3 = g_2g_4 = e$ in G_1. As a consequence, $\mathcal{F}M_1$ is a compact orientable flat surface with no cone points, hence it must be a square-tiled torus $\mathbb{R}^2/L$ where $L \subset \mathbb{Z}^2$. Furthermore, from the construction of $\mathcal{F}M$ we know that each horizontal cylinder in M corresponds to a horizontal cylinder of the same width and circumference in $\mathcal{F}M$. Hence $(2ord_G(g_1g_2), 0) \in L$. Similarly, $(0, 2ord_G(g_1g_4)) \in L$. Let M_2 be a (not necessarily connected) square tiled surface such that $\mathcal{F}M_2$ is a $2ord_G(g_1g_2)$-by-$2ord_G(g_1g_4)$

torus, then M_2 is a branched cover of M_1. By the construction of $\mathcal{F}$, M_2 is also a branched abelian cover. Furthermore, the pull back of any $\alpha' \in \mathcal{N}(M, \Sigma)$ satisfying property (L) would also satisfy property (L). Hence, we have:

Proposition 6.2.4. *Any α satisfying property (L) is related to an $\alpha_0 \in \mathcal{N}'(M_2)$ satisfying property (L) by finite branched covers, where $\mathcal{F}M_2$ is a $2ord_G(g_1g_2)$-by-$2ord_G(g_1g_4)$ torus $\mathbb{R}^2/2ord_G(g_1g_2)\mathbb{Z} \times 2ord_G(g_1g_4)\mathbb{Z}$*

□

Hence, from now on, we always let $\mathcal{F}M$ be a $2s$-by-$2t$ rectangular torus.

6.3 The discrete Fourier Transform

To apply Corollary 6.1.1, we need to find a decomposition of V that is compatible with the decomposition $H^1(M, \Sigma; \mathbb{C}) = \bigoplus_\rho H^1(\rho)$. We can obtain such a decomposition by Discrete Fourier Transform.

Let $V(\mathcal{F}M) = V(T_{s,t})$ be the space of real-valued functions on $\mathbb{Z}^2/(2s\mathbb{Z} \times 2t\mathbb{Z})$. By discrete Fourier transform, V has the following direct-sum decomposition: $V_{s,t} = \bigoplus_{\lambda,\mu} V_{s,t}^{\lambda,\mu}$, where λ, μ are integers, such that $0 \leq \lambda < s/2$, $0 \leq \mu < t$ if s is even, $0 \leq \lambda < s/2$, $0 \leq \mu < t$, or $\lambda = (s-1)/2$ and $\mu < t/2$ if s is odd, and $V_{s,t}^{\lambda,\mu} =$

$span_{\mathbb{R}}(f_{0,0}, f_{0,1}, f_{1,0}, f_{1,1}, g_{0,0}, g_{0,1}, g_{1,0}, g_{1,1})$, where:

$$f_{0,0}(x,y) = \begin{cases} \sin(2x\pi\lambda/2s)\sin(2y\pi\mu/2t), & \text{if } x+y \text{ is even} \\ 0, & \text{otherwise} \end{cases}$$

$$f_{0,1}(x,y) = \begin{cases} \sin(2x\pi\lambda/2s)\cos(2y\pi\mu/2t), & \text{if } x+y \text{ is even} \\ 0, & \text{otherwise} \end{cases}$$

$$f_{1,0}(x,y) = \begin{cases} \cos(2x\pi\lambda/2s)\sin(2y\pi\mu/2t), & \text{if } x+y \text{ is even} \\ 0, & \text{otherwise} \end{cases}$$

$$f_{1,1}(x,y) = \begin{cases} \cos(2x\pi\lambda/2s)\cos(2y\pi\mu/2t), & \text{if } x+y \text{ is even} \\ 0, & \text{otherwise} \end{cases}$$

$$g_{0,0}(x,y) = \begin{cases} \sin(2x\pi\lambda/2s)\sin(2y\pi\mu/2t), & \text{if } x+y \text{ is odd} \\ 0, & \text{otherwise} \end{cases}$$

$$g_{0,1}(x,y) = \begin{cases} \sin(2x\pi\lambda/2s)\cos(2y\pi\mu/2t), & \text{if } x+y \text{ is odd} \\ 0, & \text{otherwise} \end{cases}$$

$$g_{1,0}(x,y) = \begin{cases} \cos(2x\pi\lambda/2s)\sin(2y\pi\mu/2t), & \text{if } x+y \text{ is odd} \\ 0, & \text{otherwise} \end{cases}$$

$$g_{1,1}(x,y) = \begin{cases} \cos(2x\pi\lambda/2s)\cos(2y\pi\mu/2t), & \text{if } x+y \text{ is odd} \\ 0. & \text{otherwise} \end{cases}$$

This decomposition is related to, but not the same as the eigenspace decomposition of discrete Laplacian.

By the functorial property, the G-action on M induces an action on $\mathcal{F}M$ which in turn induces actions on various $V^{\lambda,\mu}$. More precisely, the actions of g_i on $\mathcal{F}M$, $i = 1, 2, 3, 4$, are translations in the four diagonal directions. By calculation, we know that $\Psi^{-1}(V^{\lambda,\mu}) \subset H^1(\rho^{\lambda,\mu}_{++}) + H^1(\rho^{\lambda,\mu}_{-+}) + H^1(\rho^{\lambda,\mu}_{+-}) + H^1(\rho^{\lambda,\mu}_{--})$, where the representations $\rho^{\lambda,\mu}_{\pm\pm}$ are as follows:

$$\begin{aligned}
\rho^{\lambda,\mu}_{++}(g_1) &= e^{i\pi(1+\lambda/s+\nu/t)} & \rho^{\lambda,\mu}_{++}(g_2) &= e^{i\pi(1-\lambda/s+\nu/t)} \\
\rho^{\lambda,\mu}_{++}(g_3) &= e^{i\pi(1-\lambda/s-\nu/t)} & \rho^{\lambda,\mu}_{++}(g_4) &= e^{i\pi(1+\lambda/s-\nu/t)} \\
\rho^{\lambda,\mu}_{-+}(g_1) &= e^{i\pi(1-\lambda/s+\nu/t)} & \rho^{\lambda,\mu}_{-+}(g_2) &= e^{i\pi(1+\lambda/s+\nu/t)} \\
\rho^{\lambda,\mu}_{-+}(g_3) &= e^{i\pi(1+\lambda/s-\nu/t)} & \rho^{\lambda,\mu}_{-+}(g_4) &= e^{i\pi(1-\lambda/s-\nu/t)} \\
\rho^{\lambda,\mu}_{+-}(g_1) &= e^{i\pi(1+\lambda/s-\nu/t)} & \rho^{\lambda,\mu}_{+-}(g_2) &= e^{i\pi(1-\lambda/s-\nu/t)} \\
\rho^{\lambda,\mu}_{+-}(g_3) &= e^{i\pi(1-\lambda/s+\nu/t)} & \rho^{\lambda,\mu}_{+-}(g_4) &= e^{i\pi(1+\lambda/s+\nu/t)} \\
\rho^{\lambda,\mu}_{--}(g_1) &= e^{i\pi(1-\lambda/s-\nu/t)} & \rho^{\lambda,\mu}_{--}(g_2) &= e^{i\pi(1+\lambda/s-\nu/t)} \\
\rho^{\lambda,\mu}_{--}(g_3) &= e^{i\pi(1+\lambda/s+\nu/t)} & \rho^{\lambda,\mu}_{--}(g_4) &= e^{i\pi(1-\lambda/s+\nu/t)}
\end{aligned}$$

We know that if the action of Γ on $\mathbb{P}H^1(\rho)$ for any of the space $H^1(\rho^{\lambda,\mu}_{\pm\pm})$ above is commensurable to a hyperbolic triangle group with parabolic element, then (a) $\lambda = 0$ and $\nu|t$, (b) $\nu = 0$ and $\lambda|s$, or (c) $\lambda|s$ and $\nu|t$, from the calculation in [6], [56] or Section 5.7. In the first two cases it is commensurable to the (∞, ∞, n)-triangle

group, while in case (c) it is commensurable to a (∞, m, n)-triangle group. By Corollary 6.1.1, if α satisfies property (L) then $\Psi(\alpha)$ must be in one of these two types of $V^{\lambda,\mu}$.

6.4 The (∞, ∞, n) case

In this case, without loss of generality, we can assume $\lambda = s/n$ and $\nu = 0$. Figure 6.5 shows the sign of the function $f_0 = f_{0,0} + g_{0,0}$ for $n = 5$ on vertices of $\mathcal{F}M$.

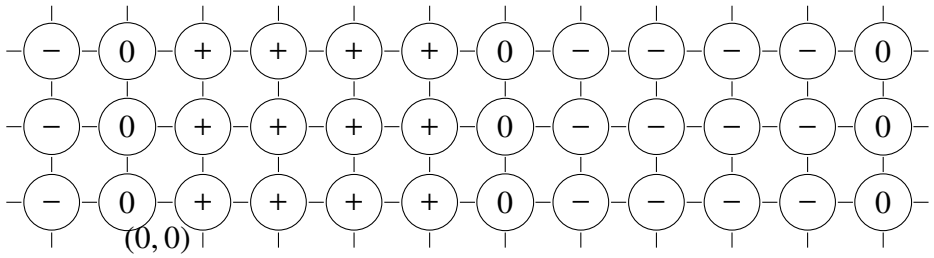

Figure 6.5: The signs on $\mathcal{F}M$ in the $(\infty, \infty, 5)$ case.

Points where $f_0 = f_{0,0} + g_{0,0}$ is positive or negative form vertical stripes, which are separated by columns of zeros, hence $\Psi^{-1}(f_0)$ defines a singular translation structure on M by Lemma 6.2.2. By computation, this translation structure is tiled by regular $2n$-gons, and $\gamma_1 r_{g_2}^{-1} f$ acts on it as a finite order rotation. These lattice surfaces were first discovered by Veech.

Now we have:

Proposition 6.4.1. *If $\alpha \in \mathcal{N}'$ that satisfies condition (L) such that $\Psi(\alpha) \in V^{s/n,0}$, then up to an affine action and an automorphism of the square-tiled surface M, $\Psi(\alpha) = f_0$. Hence, $X(\alpha)$ is tiled by regular $2n$-gons up to a $SL(2,\mathbb{R})$-action.*

Proof. Firstly, because the sum of the values of $\Psi(\alpha)$ is 0, by Lemma 6.2.2, the set of vertices where $\Psi(\alpha)$ is positive and the set of vertices where $\Psi(\alpha)$ is negative have to be separated by vertices where $\Psi(\alpha)$ is 0. Hence, $\Psi(\alpha)$ must reach 0 at a certain vertex. After relabeling the vertices if necessary, we can assume $\Psi(\alpha)$ is 0 at $(0,0)$ without loss of generality. Hence $\Psi(\alpha)(-1,1)\Psi(\alpha)(1,1) < 0$ or $\Psi(\alpha)(x,y) = 0$ for all $x+y$ even. If $\Psi(\alpha)(-1,1)\Psi(\alpha)(1,1) < 0$, by Lemma 6.2.2, $\Psi(\alpha)(0,1) = 0$, hence $\Psi(\alpha)(x,y) \in f_{0,0}\mathbb{R} + g_{0,0}\mathbb{R}$, thus α is affine equivalent to α_0.

The other case, $\Psi(\alpha)(x,y) = 0$ for all $x+y$ even, contradicts with our assumption according to Lemma 6.2.2. □

6.5 The (∞, m, n) case, Bouw-Möller surfaces

Now we deal with the (∞, m, n) case. Let $f_1 = f_{0,0} + g_{0,0}$. Points where f_1 is positive or negative form rectangles, which are separated by columns and rows of zeros, hence $\Psi^{-1}(f_1)$ defines a singular translation structure on M by Lemma 6.2.2. Figure 6.6 shows the sign of f_1 when $m = 5, n = 3$.

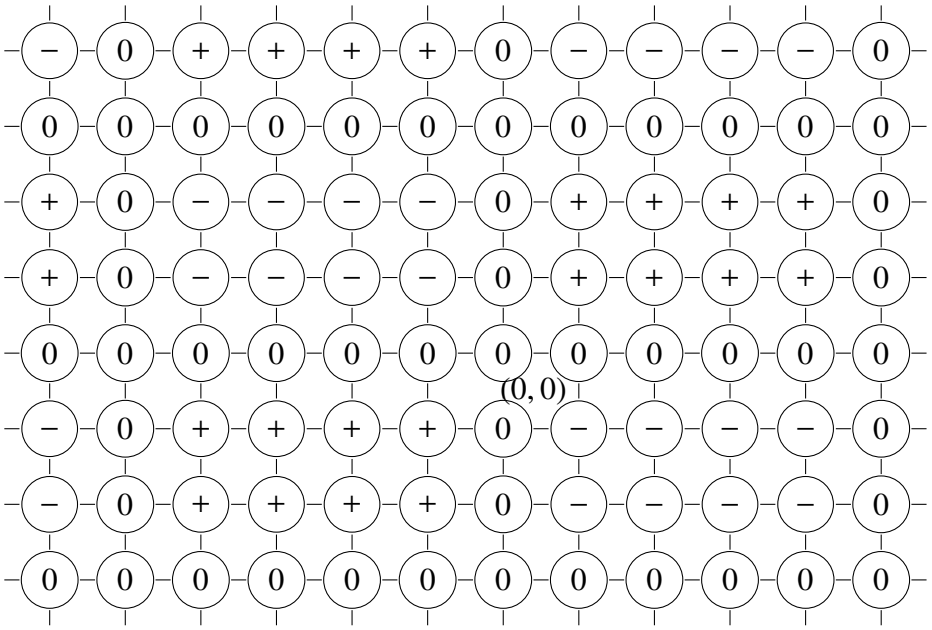

Figure 6.6: The signes on $\mathcal{F}(M)$ in the $(\infty, 5, 3)$ case.

By deleting vertices that are assigned 0 width in the 1-skeleton on $T_{s,t}$ we can get the grid graph described in [27], hence due to Lemma 6.2.1, the metric completion of each component of $(X(\Psi^{-1}(f_1)) - \Sigma')_*$ is the (m, n) Bouw-Möller surface. Affine maps $\gamma_1 r_{g_2}^{-1} f$ and $\gamma_2 t^2 r_{g_4 g_1} f$ act on it as finite order rotations.

For example, if we label the squares of $\mathcal{F}M$ in the Figure 6.6 above as in Figure 6.7, then one component of $X(\Psi^{-1}(f_1))$ becomes Figure 6.8, and $X(\Psi^{-1}(f_1))$ is a union of copies of such translation surfaces glued together at the cone point.

Also, when $m = n$, $f_2 = f_{0,0} + f_{1,1} + g_{0,0} + g_{1,1}$ and $f_3 = f_{0,1} + f_{0,1} + g_{1,0} + g_{1,0}$

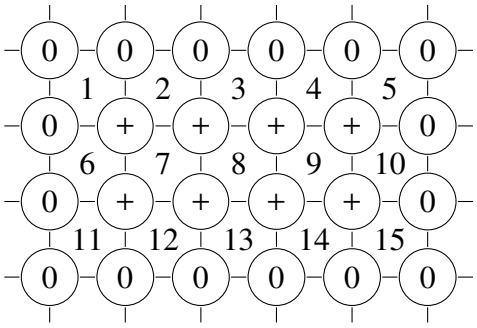

Figure 6.7: Squares in $\mathcal{F}(M)$.

also define lattice surfaces. They are affine equivalent to branched covers of the regular n-gon branched at the midpoints of its sides. Figure 6.9 shows the sign of f_2 for $m = n = 5$, and Figure 6.10 shows the corresponding translation surface.

Similar to the previous section, we have:

Proposition 6.5.1. *If $\alpha \in \mathcal{N}'$ that satisfies condition (L) such that $\Psi(\alpha) \in V^{s/n,t/m}$, then up to affine action and the automorphism of M, $\Psi(\alpha)$ is either f_1 or f_2.*

Proof. Due to Lemma 6.2.1, we can further assume that $A\Psi(\alpha) = \lambda\Psi(\alpha)$ for some constant λ. From this and the Peron-Frobenious theorem we know that the sign of $\Psi(\alpha)$ completely determines $\Psi(\alpha)$ up to scaling.

By the formula for $f_{i,j}$ and $g_{i,j}$, $i, j = 0, 1$ in Section 6.3 and the fact that $A\Psi(\alpha) = \lambda\Psi(\alpha)$, $\Psi(\alpha) = C_1 \sin(\pi x/n + A)\cos(\pi y/m) + C_2 \sin(\pi x/n + B)\sin(\pi y/m)$ for some constants C_1, C_2, A and B. Hence, $\Psi(\alpha)$ when restricted to any row is a

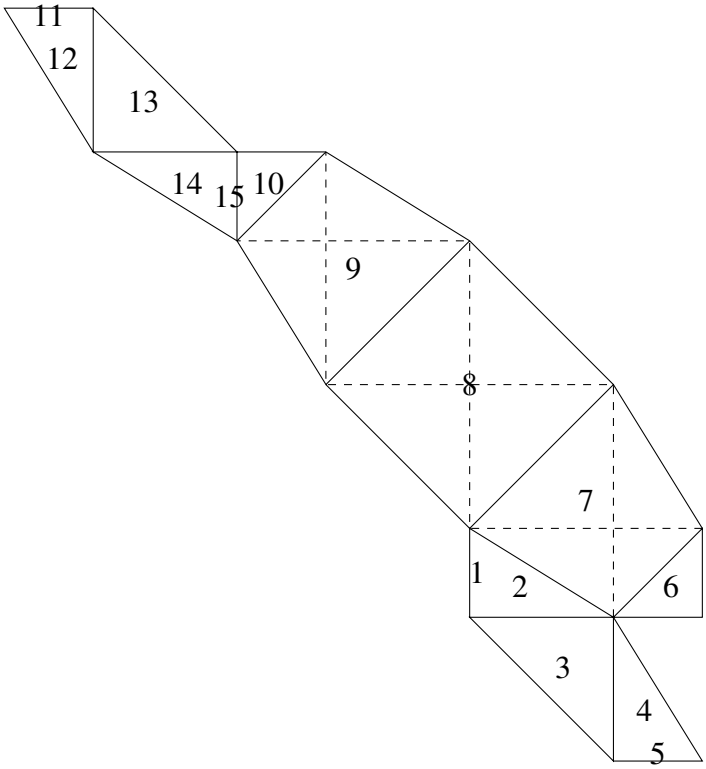

Figure 6.8: Squares in Figure 6.7 after flipping and deformation.

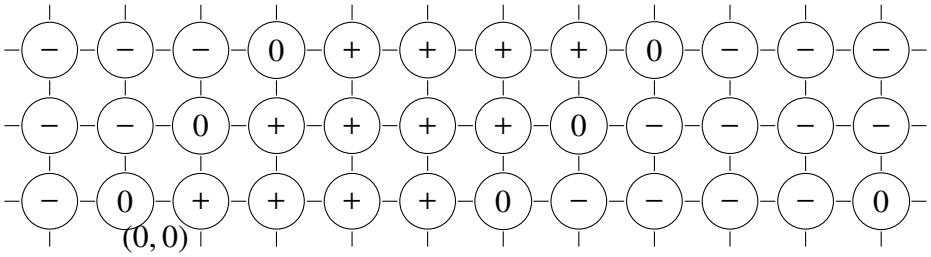

Figure 6.9: Another width function.

function of the form $\psi(x) = C\sin(\pi x/n + a)$ for some constants C and a, and when restricted to any column it is a function of the form $\psi'(x) = C'\sin(\pi y/m + a')$ for some constants C' and a'. Furthermore, by Lemma 6.2.2, the set of vertices where $\Psi(\alpha)$ is positive and the set of vertices where $\Psi(\alpha)$ is negative have to be separated

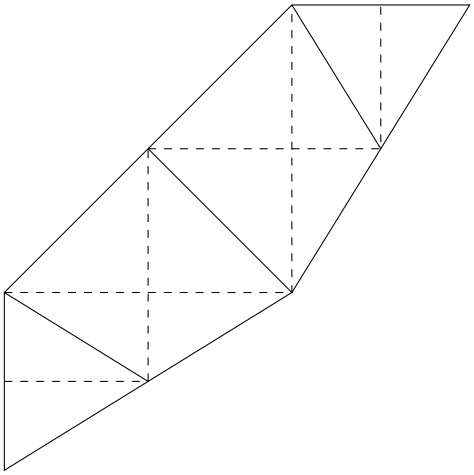

Figure 6.10: The surface obtained from Figure 6.9.

by vertices where $\Psi(\alpha)$ is 0. Hence, $\Psi(\alpha)$ restricted to any row of vertices must be one of the following cases:

(a) 0.

(b) $C\sin(\pi(x-k)/n)$, $k \in \mathbb{Z}$. It reaches 0 $\frac{2s}{n}$ times.

Similarly, $\Psi(\alpha)$ restricted to any column of vertices must be one of the following cases:

(a) 0.

(b) $C'\sin(\pi(x-k')/m)$, $k' \in \mathbb{Z}$. It reaches 0 $\frac{2t}{m}$ times.

Because of Lemma 6.2.2, at least one row or column must be in case (b). Furthermore, we have:

Lemma 6.5.2. *If a row (or column) of type (a) is next to a row (or column) of type (b), the subgraph spanned by vertices where $\Psi(\alpha)$ is non-zero is a union of grid graphs as defined in [27]. Hence, it must be a cover of a Bouw-Möller surface.*

Proof. If a row of type (a) is next to a row of type (b), without loss of generality, we let the row of type (a) be the 0-th row, and the row of type (b) be the 1st. Because $\Psi(\alpha) = C_1 \sin(\pi x/n + A)\cos(\pi y/m) + C_2 \sin(\pi x/n + B)\sin(\pi y/m)$ and $\Psi(\alpha)(x, y) = 0$, $C_1 = 0$. Furthermore, because the 1st row is of type (b), $nB/\pi \in \mathbb{Z}$. Hence the subgraph spanned by vertices where $\Psi(\alpha)$ is non-zero is a union of grid graphs as defined in [27]. The argument for columns is the same. □

Now we only need to deal with the case when $\Psi(\alpha)$ restricted to all rows and columns of vertices are of type (b). Because all columns are of type (b) there must be $\frac{4st}{m}$ zeros, and because all rows are of type (b) there must be $\frac{4st}{n}$ zeros. Hence, $m = n$. Now, the only way these zero vertices can separate the other vertices of $T_{s,t}$ into positive and negative regions is by aligning in the diagonal direction.

In conclusion, after scaling and relabeling, $\Psi(\alpha)$ must be either $f_{0,0} + f_{1,1} + g_{0,0} + g_{1,1}$ or $f_{0,1} + f_{0,1} + g_{1,0} + g_{1,0}$. □

Proof of Theorem 6.1.1. Theorem 6.1.1 is a corollary of Proposition 6.4.1 and Proposition 6.5.1. □

BIBLIOGRAPHY

[1] Jayadev S Athreya and Jon Chaika. The distribution of gaps for saddle connection directions. *Geometric and Functional Analysis*, 22(6):1491–1516, 2012.

[2] Jayadev S Athreya, Jon Chaika, and Samuel Lelievre. The gap distribution of slopes on the golden *l. Contemp. Math*, 631:47–62, 2015.

[3] Matt Bainbridge, Philipp Habegger, and Martin Moeller. Teichmüeller curves in genus three and just likely intersections in $G_m^n \times G_a^n$. *arXiv preprint arXiv:1410.6835*, 2014.

[4] Matt Bainbridge and Martin Möller. The Deligne-Mumford compactification of the real multiplication locus and Teichmüller curves in genus 3. *Acta mathematica*, 208(1):1–92, 2012.

[5] Matt Bainbridge, John Smillie, and Barak Weiss. Horocycle dynamics: new invariants and eigenform loci in the stratum $\mathcal{H}(1,1)$. *arXiv preprint arXiv:1603.00808*, 2016.

[6] I. I. Bouw and M. Möller. Teichmüller curves, triangle groups, and Lyapunov exponents. *Ann. of Math.*, 172(2):139–185, 2010.

[7] Jean-Luc Brylinski. *Loop spaces, characteristic classes and geometric quantization*. Springer, 1993.

[8] Kariane Calta. Veech surfaces and complete periodicity in genus two. *Journal of the American Mathematical Society*, 17(4):871–908, 2004.

[9] H. S. M. Coxeter. *Regular Polytopes*. Dover Publications, 1973.

[10] JS Dani. Density properties of orbits under discrete groups. *J. Indian Math. Soc*, 39:189–218, 1975.

[11] Vincent Delecroix. Flatsurf package of sagemath. `http://www.labri.fr/perso/vdelecro/flatsurf.html`.

[12] P. Deligne and G. D. Mostow. Monodromy of hypergeometric functions and non-lattice integral monodromy. *Publications Mathématiques de l'IHÉS*, 63(1):5–89, 1986.

[13] L. E. Dickson. *Algebraic Theories*. Dover Publications, 1959.

[14] A. Eskin, M. Konstevich, and A. Zorich. Lyapunov spectrum of square-tiled cyclic covers. *Journal of modern dynamics*, 5(2):319–353, 2011.

[15] Alex Eskin, Jens Marklof, and Dave Witte Morris. Unipotent flows on the space of branched covers of veech surfaces. *Ergodic Theory and Dynamical Systems*, 26(01):129–162, 2006.

[16] Alex Eskin and Howard Masur. Asymptotic formulas on flat surfaces. *Ergodic Theory and Dynamical Systems*, 21(02):443–478, 2001.

[17] Alex Eskin, Howard Masur, Martin Schmoll, et al. Billiards in rectangles with barriers. *Duke Mathematical Journal*, 118(3):427–464, 2003.

[18] Alex Eskin, Howard Masur, and Anton Zorich. Moduli spaces of abelian differentials: the principal boundary, counting problems, and the Siegel-Veech constants. *Publications Mathématiques de l'Institut des Hautes Études Scientifiques*, 97:61–179, 2003.

[19] Alex Eskin, Maryam Mirzakhani, and Amir Mohammadi. Isolation, equidistribution, and orbit closures for the $SL(2,\mathbb{R})$ action on Moduli space. *Annals of Mathematics*, 182(2):673–721, 2015.

[20] G. Forni. On the Lyapunov exponents of the Kontsevich-Zorich cocycle. In *Handbook of Dynamical Systems*. Elsevier, 2006.

[21] G. Forni and C. Matheus. An example of a Teichmüller disk in genus 4 with degenerate Kontsevich-Zorich spectrum. 2008. arXiv preprint arXiv:0810.0023.

[22] G. Forni, C. Matheus, and A. Zorich. Square-tiled cyclic covers. *J. Mod. Dyn.*, 5:285–318, 2011.

[23] Ralph H. Fox and Richard B. Kershner. Concerning the transitive properties of geodesics on a rational polyhedron. *Duke Mathematical Journal*, 2:147–150, 1936.

[24] Allen Hatcher. *Algebraic Topology*. Cambridge University Press, 2002.

[25] F. Herrlich and G. Schmithüsen. An extraordinary origami curve. *Math. Nachr.*, (2):219–237.

[26] Fritz Herzog and BM Stewart. Patterns of visible and nonvisible lattice points. *American Mathematical Monthly*, pages 487–496, 1971.

[27] W. P. Hooper. Grid graphs and lattice surfaces. *International Mathematics Research Notices*, 12, 2013.

[28] P. Hubert and G. Schmithüsen. in preparation.

[29] Richard Kenyon and John Smillie. Billiards on rational-angled triangles. *Commentarii Mathematici Helvetici*, 75(1):65–108, 2000.

[30] Erwan Lanneau and Duc-Manh Nguyen. Teichmüller curves generated by Weierstrass Prym eigenforms in genus 3 and genus 4. *Journal of Topology*, page jtt036, 2013.

[31] Erwan Lanneau, Duc-Manh Nguyen, and Alex Wright. Finiteness of Teichmüller curves in non-arithmetic rank 1 orbit closures. *arXiv preprint arXiv:1504.03742*, 2015.

[32] Christopher J Leininger. On groups generated by two positive multi-twists: Teichmüller curves and Lehmers number. *Geometry & Topology*, 8(3):1301–1359, 2004.

[33] Howard Masur. Interval exchange transformations and measured foliations. *Annals of Mathematics*, 115(1):169–200, 1982.

[34] Howard Masur. Lower bounds for the number of saddle connections and

closed trajectories of a quadratic differential. In *Holomorphic Functions and Moduli I*, pages 215–228. Springer, 1988.

[35] Howard Masur. The growth rate of trajectories of a quadratic differential. *Ergodic Theory and Dynamical Systems*, 10(01):151–176, 1990.

[36] Carlos Matheus and Alex Wright. Hodge-Teichmüller planes and finiteness results for Teichmüller curves. *Duke Mathematical Journal*, 164(6):1041–1077, 2015.

[37] Carlos Matheus and Jean-Christophe Yoccoz. The action of the affine diffeomorphisms on the relative homology group of certain exceptionally symmetric origamis. *Journal of Modern Dynamics (JMD)*, 4(3):453–486, 2010.

[38] C. T. McMullen. Braid groups and Hodge theory. *Mathematische Annalen*, 355(3):893–946, 2013.

[39] Curtis T McMullen. Teichmüller curves in genus two: Discriminant and spin. *Mathematische Annalen*, 333(1):87–130, 2005.

[40] Curtis T McMullen. Prym varieties and Teichmüller curves. *Duke Mathematical Journal*, 133(3):569–590, 2006.

[41] Curtis T McMullen. Dynamics of over Moduli Space in Genus Two. *Annals of mathematics*, pages 397–456, 2007.

[42] Curtis T McMullen et al. Moduli spaces of isoperiodic forms on Riemann surfaces. *Duke Mathematical Journal*, 163(12):2271–2323, 2014.

[43] Yair Minsky and Barak Weiss. Cohomology classes represented by measured foliations, and Mahlers question for interval exchanges. *Ann. Scient. Éc. Norm. Sup.*, 4(47):245–284, 2014.

[44] G. Schmithüsen. An algorithm for finding the Veech group of an origami. *Experimental Mathematics*, 13(4):459–472, 2004.

[45] Marjorie Senechal. What is a quasicrystal. *Notice of the AMS*, 53:886–887, 2006.

[46] J-P Serre. *Linear representations of finite groups*. 1977.

[47] J. Smillie and B. Weiss. Examples of horocycle-invariant measures on the moduli space of translation surfaces.

[48] John Smillie and Barak Weiss. Minimal sets for flows on moduli space. *Israel Journal of Mathematics*, 142(1):249–260, 2004.

[49] John Smillie and Barak Weiss. Characterizations of lattice surfaces. *Inventiones mathematicae*, 180(3):535–557, 2010.

[50] W. P. Thurston. Shapes of polyhedra and triangulations of the sphere. *Geometry and Topology Monographs*, 1:511–549, 1998.

[51] William P Thurston et al. On the geometry and dynamics of diffeomorphisms of surfaces. *Bulletin (new series) of the American Mathematical Society*, 19(2):417–431, 1988.

[52] William A Veech. Teichmüller curves in moduli space, Eisenstein series and an application to triangular billiards. *Inventiones mathematicae*, 97(3):553–583, 1989.

[53] Yaroslav B. Vorobets. Planar structures and billiards in rational polygons: the Veech alternative. *Russian Mathematical Surveys*, 51(5):779–817, 1996.

[54] Clayton C Ward. Calculation of fuchsian groups associated to billiards in a rational triangle. *Ergodic Theory and Dynamical Systems*, 18(04):1019–1042, 1998.

[55] A. Wright. Schwarz triangle mappings and Teichmüller curves: abelian square-tiled surfaces. *J. Mod. Dyn.*, 6(3):405–426, 2012.

[56] A. Wright. Schwarz triangle mappings and Teichmüller curves: the Veech-

Ward-Bouw-Möller curves. *Geometric and Functional Analysis*, 23(2):776–809, 2013.

[57] Alex Wright. Translation surfaces and their orbit closures: An introduction for a broad audience. *arXiv preprint arXiv:1411.1827*, 2014.

[58] Yumin Zhong. On the areas of the minimal triangles in Veech surfaces.

[59] Anton Zorich. Flat surfaces. In *Frontiers in number theory, physics, and geometry I. On random matrices, zeta functions, and dynamical systems. Papers from the meeting, Les Houches, France, March 9–21, 2003*, pages 439–585. Springer, 2006.